Referee #1
Manuscript: ACP-2019-829 (Yu et al.) Title: The isotopic composition of atmospheric nitrous oxide observed at the high-altitude research station Jungfraujoch, Switzerland.
This manuscript presents measurements of the isotopic composition of N_2O obtained from a high-altitude European site – Jungfraujoch in Switzerland, using a recently developed QCLS coupled with a preconcentration unit. The system provided direct and individual measurements of four N_2O isotopocules at an ambient level of N_2O. From the extensive data sets covering the 5-year study period, authors attempt to derive seasonality and interannual trends in N_2O isotopic compositions and discuss them in combination with observed changes in N_2O mixing ratio. Overall, the writing and figures are clear, and the methodology maximizes the functionality of a high-quality dataset. I encourage the publication of this important work, with only a few minor considerations/edits suggested below.

1. LN 186: Sphinx observatory→ Sphinx observatory in the Jungfraujoch station

R: OK

2. LN 357-364: Authors determined annual growth rates of N_2O mixing ratio for all in-situ data from 2014 to 2018, with/without the 2014 GC-ECD data, and free tropospheric data only, respectively. Given their 1-sigma values, it seems there are some discrepancies between the entire dataset vs sub-sets of data. Authors did mention some about those discrepancies in lines 548-553. However, if authors thought that they are statistically significant, then additional explanations should be given here, rather than later.
R: Thanks for the suggestion. In section 3.1, we have further elaborated this: "This difference in N_2O growth rates is probably due to the limited data quality of GC-ECD, although a lower growth rate in 2014 compared to 2015-2018 cannot be excluded.".

3. LN 375-380: The observed, de-seasonalized trends of delta15N_SP for the whole dataset increased, while delta15N_SP trend showed a decrease when PBL-influenced air samples were excluded. So, authors stated that it implies an impact of local sources. Does it mean that the potential local sources have high delta15N_SP signals? What could it be? Based on the two-box model approach using the current data, authors determined the average isotopic signatures for anthropogenic sources were lower than those for the background troposphere (LN 394-397). If so, the local sources mentioned above could not be associated with anthropogenic sources?
R: The authors agree, that the increasing trend of $d^{15}N^{SP}$ observed between April 2014 and December 2018 at Jungfraujoch (Fig. 2) and the decreasing trend over longer timescales as derived with a two-box modelling approach using the EDGAR emission inventory (Fig. 6; original version) might look inconsistent.
However, it is noteworthy that, the deseasonalized trends of $\delta^{15}N^{SP}$ at Jungfraujoch were not statistically significant, with/without filtering for impact from planetary boundary layer (LN 375-377_Original version). The only significantly positive trend of $\delta^{15}N^{SP}$ was found in the first phase (Table 1). Although mean $\delta^{15}N^{SP}$ values of N_2O sources according to EDGAR emission inventory are lower than that observed in tropospheric background (Table S2), a changing proportion of N_2O-emitting soil process, i.e. nitrification vs. denitrification, with $\delta^{15}N^{SP}$ values of 33‰, as compared to about 0‰ (Sutka et al., 2006), might rationalize this inconsistency. This shift in the

isotopic signatures of anthropogenic sources, might be interpreted as a climate change feedback, as discussed in section 4.4. Similarly, Park et al. (2012) attributed an increase rate of 0.06‰ a^{-1} in $\delta^{15}N^{SP}$ in 2005 to 10% increase in the relative contribution of nitrification to global N_2O production since 1975. This is already discussed in section 4.3.
In the two-box model approach, the estimation of isotopic signatures for anthropogenic sources mainly depends on the measured current and predefined preindustrial N_2O mixing ratios and isotopic signatures (Table S1). As shown in Figure 6 (original version), the simulated trend of $\delta^{15}N^{SP}$ in the troposphere is negative, consistent with the lower $\delta^{15}N^{SP}$ for anthropogenic sources than for the tropospheric background. The current (insignificant) increase in $d^{15}N^{SP}$ at Jungfraujoch, might be evaluated with the two-box model approach in the future, if extended time-series of isotope data will become available (e.g. Prokopiou et al., 2017).

4. LN 405-409: Authors found that there were differences in seasonal patterns of all isotopes between the entire dataset vs. the second phase data. Authors then added that the seasonal variations for free tropospheric samples were similar to those for the whole dataset. Does it imply that the second phase patterns could more represent the PBL-influenced data?
R: As indicated in LN 401-409 (original version) and Figure 3, we found a significant seasonal pattern of $\delta^{15}N^{SP}$, with a summer minimum, for both the whole dataset and the second phase. For $\delta^{15}N^{bulk}$, a significant seasonal pattern was seen in the whole dataset but not in the second phase (seasonal variability > uncertainty). Hence, our results do not necessarily indicate that seasonal patterns were different between the entire and the second-phase data.
Air mass footprints suggest that, in 2017 (second phase), discrete sampling received less contribution from free troposphere than in the other years (Fig. 4b), possibly pointing to a stronger influence of PBL. However, this is not supported by *in situ* NO_y and CO measurements (Figure S6b; no clear difference), which has been suggested as a more effective indicator for free troposphere (Herrmann et al., 2015). Given the larger uncertainty in seasonality-analysis due to lower sampling frequency in the second phase (Section 3.4), it is difficult to draw the conclusion that such "insignificant" changes in seasonal patterns in the second phase are due to a stronger PBL influence.

5. LN 421-428: Authors seem to suggest strong exchange with the PBL in summer, based on the observed summer maxima in the monthly seasonal cycles for O_3 and NO_y mixing ratios. But it is not so clear that the summer maxima in O_3 and NO_y could support a stronger air mixing with the surface and thus a PBL impact on the seasonal changes in N_2O isotopic compositions, because the maxima in O_3 and NO_y mixing ratio occur in summer most likely due to stronger sunlight.
R: We agree that O_3 alone may not be a good indicator for air exchange with PBL, as elevated O_3 concentration at Jungfraujoch can be due to air exchange with PBL and/or stratosphere. Therefore, the text in section 3.4 has now been revised. However, NO_y : CO used in this study has been previously tested to be an effective indicator for determining the age of air mass, i.e. to identify recently polluted air transported to Jungfraujoch from the PBL (Herrmann et al., 2015; Zellweger et al., 2003). In addition, air mass footprint analysis supports such pattern with lowest source sensitivity from free troposphere in summer (Figure 4).

6. LN 453-476: In the results section, authors analyzed the seasonal variabilities for not only the entire datasets but also the second phase data, but in the seasonality discussion, the seasonal patterns derived from the second phase data were not discussed, even though the second phase

patterns might contains more the surface-influenced signals (see the comment #4). If authors decided not to consider the second phase seasonality, please add statements for the reason in the text.

R: For the second phase, the seasonal patterns of $\delta^{15}N^{bulk}$ and $\delta^{18}O$ were not significant, while $\delta^{15}N^{SP}$ showed a significant seasonal pattern similar to that for the whole dataset. Therefore, it was not specifically discussed. Nonetheless, we thank the reviewer for the suggestion and have added a few more discussion points in section 4.2, regarding the seasonal variabilities of N_2O isotopic signature in the second phase.

7. LN 488-505: Fig. 5 demonstrated that direct/indirect agricultural source contributes most to the N_2O enhancements, particularly in summer. Then considering peak N_2O fluxes and minimum of delta15N_SP observed in summer, does it suggest that the local agricultural activities enhanced N_2O production by "denitrification"? Are there any studies to support this result?

R: Yes, one isotopic study of N_2O emissions from Swiss grassland (Wolf et al., 2015) suggested that N_2O emissions in summer periods were mostly contributed by denitrification, given that high N_2O fluxes were associated with low $\delta^{15}N^{SP}$ values (below 5‰). This has been confirmed again in a recent study (Ibraim et al., submitted to Global Biogeochemical Cycles) showing that the $\delta^{15}N^{SP}$ of N_2O emitted from a managed grassland during a late summer was consistently within a small range of 0-10‰, regardless of soil water-filled-pore-space.

Referee #2
Review on "**The isotopic composition of atmospheric nitrous oxide observed at the high-altitude research station Jungfraujoch, Switzerland**".

This manuscript described the 5-year observations of nitrous oxide (N_2O) mixing ratios and their isotopic compositions at Jungfraujoch using laser spectroscopic technique for the first time. The long-term observations of N_2O isotopocules allow the authors to characterize the integrated isotopic signatures of anthropogenic sources that have been emitted since the industrial revolution and to identify the main processes governing the seasonality of N_2O. The authors utilized a two-box model and a Lagrangian particle dispersion model to characterize the isotope signatures of anthropogenic sources that contribute to the atmospheric increase of N_2O concentration. The unique observations of N_2O isotopocules in the middle of the European continent and the interesting interpretation of data makes worth publication. Notwithstanding, there are several hazy spots in the manuscript which needs to be revised in order to avoid any confusion.

Major issues:
1. Application of a two-box model assumes the data obtained at Jungfraujoch to represent the variability of N_2O mixing ratios and its isotopocules in the troposphere. This appear to contradict to the use of footprint model to characterize the isotopic signatures of the anthropogenic sources in the European continent. This is demonstrated in Table 2 and 3 that the isotopic signatures of the anthropogenic N_2O are different. In the text on the lines from 626 to 635, the authors ascribed it to the different isotopic signatures of N_2O source emissions in the model. However, as shown in Table 2 and mentioned in the text (on the line of 612), the single spot observation won't be representative the global scale of atmosphere, but would represent the regional characteristics of N_2O. The long-term trends of N_2O isotopocules listed in Table 1 also support that the observation at Jungfraujoch does not represent the tropospheric variability of N_2O. Contradict to the global trends of isotopocules shown in Figure 6, the observations of $\delta^{15}N^{SP}$ and $\delta^{18}O$ are positive trends at Jungfraujoch. In view of these contradict aspects revealed in the observation and the model, the isotopic signatures of the anthropogenic source will not help understand the contribution of anthropogenic source to the increase of atmospheric N_2O. I would suggest limiting the data interpretation in regional scale.
R: We thank the review for the critics and suggestions. Although the reviewer suggests to limit our data interpretation with respect to the global model, we argue that the air samples collected from Jungfraujoch Sphinx still represent the background troposphere, despite the contribution of regional emissions to the seasonal variability. The box model estimates for the emission strength and isotopic composition of the anthropogenic source are largely depending on the mean values of N_2O concentrations and isotopic composition at Jungfraujoch, and little affected by subtle temporal changes, which are shown in the seasonal variabilities. Based on the NO_y : CO criterion (Herrmann et al., 2015; Zellweger et al., 2003), which has been identified as an effective indicator for the (short) age of air mass, 110 out of 142 sample points were found to represent the free troposphere. To demonstrate that two-box model results are not affected by regional emissions, we re-ran the two-box model with the data filtered for free troposphere and got statistically identical results. The new results are now mentioned in section 4.4.
Regarding the reviewer's arguments referring to Table 2 and 3 as well as the texts in discussion, we believe that there are misinterpretations. In our discussion (LN 626-635), the differences in source isotopic signatures between Table 2 (two-box model) and Table 3 (bottom-up estimate) was

largely attributed to the uncertainty in the estimated source isotopic signatures, which were used in the bottom-up model (Table S2; original version). This was further explained by comparing our bottom-up estimates with those from Toyoda et al. (2013), demonstrating that the selection of source isotopic signatures for distinct source categories from literature largely influence the isotopic composition of the anthropogenic source.

We are aware that a single-site study can be limited in determining long-term trends of N_2O isotopic signatures. As we discussed in the manuscript, extension of the study period at an even higher sampling frequency would reduce such uncertainties. Although the interannual trends of $\delta^{15}N^{SP}$ and $\delta^{18}O$ were positive in the first phase of our observation, we obtained insignificant trends for the whole dataset, which in return makes a minor influence on the model estimates. Given the relatively short study period, the mean isotopic signatures observed at Jungfraujoch is more important than the trends for determining isotopic signatures of anthropogenic sources from the NH background atmosphere.

2. The long-term observation at one station allowed seasonal variation to be explored. The authors argued the minimum N_2O concentration observed in late summer is driven by STE which is also evidenced by the enrichment of ^{15}N in the N_2O driven by the photochemical destruction in the stratosphere. On the other hand, $\delta^{15}N^{SP}$ and $\delta^{18}O$ did not seemingly synchronize the STE event, which, the authors argued, the N_2O emitted from the soil overwhelms the effect by STE. If these two processes govern the seasonality of the atmospheric N_2O, I would suggest quantifying how to compete these two processes along the year at Jungfraujoch.

R: The authors agree, as already mentioned in the manuscript, that N_2O isotopic composition at Jungfraujoch is controlled by stratospheric intrusions and uplift of polluted air masses. However, it is currently not possible to quantify the relative importance of these two mechanisms over time, given that temporally resolved isotopic signatures of stratospheric air and soil N_2O sources are not available for Jungfraujoch. We simulated the contribution of upper tropospheric air (15 km) to Jungfraujoch station, which is highest in the August. This acts as a qualitative indicator of the seasonal pattern of STE, which assists to explain the seasonal variability of $\delta^{15}N^{bulk}$ (added to the discussion 4.2). On the other hand, simulations of N_2O enhancements (on average 60% from soil) for 2017-2018 suggest that ground emissions of N_2O were highest in the early to middle summer (Fig. 5; original version). In August, when N_2O mixing ratios were lowest below baseline, the N_2O depletion due to mixing with stratospheric air clearly outcompeted the enhancement from ground emissions.

In a back-of-the-envelope calculation, we assume N_2O enhancement from ground-based emissions in August to be 0.15-0.20 nmol mol^{-1}, which is close with or slightly smaller than the maximum change of N_2O mixing ratio above baseline (0.20 nmol mol^{-1}; Fig. 1b). Then, given that the net minimum of N_2O mixing ratio in August is -0.2 nmol mol^{-1} below baseline, we can estimate the N_2O depletion due to STE as 0.35-0.40 nmol mol^{-1}. In addition, N_2O enhancement by soil emission (60% of total ground emission) can be calculated as 0.09-0.12 nmol mol^{-1}. With the isotopic effect associated with each mechanism from literature, we may estimate the combined effects of the two mechanisms on the maximum variabilities of $\delta^{15}N^{SP}$ in the late summer at Jungfraujoch. The net isotopic effect of mixing with stratospheric air is assumed to be about +5‰ for the lower stratosphere (higher isotopic signature but smaller mixing ratio for higher stratosphere) (Toyoda et al., 2018); the isotopic effect due to switch from nitrification to denitrification is assumed to be -30‰ (Sutka et al., 2006). Therefore, STE contributes N_2O depletion at a strength four times of that from soil emissions, while the isotopic effect of STE is only 1/6. Based on the estimates above,

it is reasonable to suggest that soil emission would outcompete STE in regulating $\delta^{15}N^{SP}$ during the late summer. Nevertheless, our estimates may have large uncertainty, and require further validation with isotopic measurements of two individual processes. By contrast, given that the isotopic effects of soil processes are much smaller for $\delta^{15}N^{bulk}$ (Toyoda et al., 2011), STE stands out to control the variability of $\delta^{15}N^{bulk}$ during late summer. We have now implemented these estimates in the supplementary material and have included more discussion in the manuscript.

02
Minor issues and technical comments:
1. L 52: The publication year of Tian et al. (2018) is 2019.
2. L 171: "gas chromatography" should be "gas chromatograph" in the context.
R: OK.

3. L 170 – 184: Since no references are given, I suggest describing the analytical methods in detail including the calibration of the system for the analysis of N_2O, CO, NO_y, and O_3 mole fractions perhaps in the section of Supporting Information.
R: Thanks for the suggestion. Additional details on the analytical method of N_2O is now implemented. The references for CO, NO_y and O_3 were given in the section 2.1 for atmospheric pollutant measurements at Jungfraujoch. In the revision, we have referred to specific publications for each pollutant giving more details on analytical methods.

4. L 217: Have you tested the mole fraction dependency of the isotope ratios of N_2O? Here, the amount of N_2O for the QCL is 45 ppm. However, Mohn et al. (2010, 2012) concentrated ambient air to > 60 ppm of N_2O.
R: Yes. The dependency of N_2O mole fraction on isotopic results was determined and corrected for (if necessary) during every batch of measurement. In addition, following identical-treatment principle, we fixed the N_2O mole fractions of calibration standards (CG1 and CG2) to the same level 45 ppm.

5. L 218: I think the citation of Harris et al. (2017) should be Harris et al. (2014).
R: Not true. Harris et al. (2014) described the laser spectroscopic technique that was developed in MIT for N_2O isotopic measurement; however, this study shares the same instrumentation as Harris et al. (2017) which was developed at Empa (Switzerland).

6. L 236: What are the matrix gases in CG1 and CG2 standards?
R: 78% N_2 and 21% O_2. This is now mentioned in the manuscript.

7. L 253: In Figure S2, the scattering of isotope ratios in the second phase look larger than that in the first phase, particularly for $\delta^{18}O$. Is it statistically insignificant?
R: Statistically, the difference is not significant.

8. L 313 – 314: T_{PI} and T_{PD} should be replaced to τ_{PI} and τ_{PD}.
R: OK

9. L 353: It's misleading. Fig. S3 shows the agreement improved since the year 2015 when GC-ECD was replaced to OA-ICOS, NOT in the second phase.

R: This is now revised. See section 3.1 for change.

10. L 358 – 361: Provide the ground that the N_2O growth rates of 0.880±0.001, 0.993±0.001, and 0.93 are in agreement. Statistically they are different each other unless standard deviation of the global growth rate of 0.93 (by NOAA) is larger than ~0.02.
R: We agree. The uncertainty of growth rates by NOAA is around 0.03 nmol mol^{-1} a^{-1}, suggesting that the global mean growth rate of 0.93 ± 0.03 nmol mol^{-1} a^{-1} is lower than retrieved from our measurements at Jungfraujoch, excluding GC-ECD measurements (2015-2018). This is now revised.

11. L 361: Add the literature (WMO, 2018) next "NOAA (0.93 nmol mol^{-1} a^{-1})".
R: OK.

12. L 362 – 364: The annual growth rate, 0.813±0.027 is not lower than the value 0.858±0.002 within 2 standard deviations.
R: This is now revised as "the absolute growth rate determined from the discrete gas samples was even lower albeit larger uncertainty (0.813 ± 0.027 nmol mol^{-1} a^{-1})".

13. L 376: The authors indicate the insignificant increasing trend of $\delta^{15}N^{SP}$ and $\delta^{18}O$. However, their standard deviations do suggest significant increase of them within 1 sd. It needs to be clarified.
R: In Table 1, we showed coefficients from linear regressions with 1 SD. However, as indicated in section 2.6, significance level for linear regression was set to $p < 0.01$ (confidence level of 99%). Hence, this would require coefficients to be larger than 3 times of SD.

14. L 383 – 391: It needs explanation why the trends of $\delta^{15}N^{SP}$ and $\delta^{18}O$ during the first phase is one order of magnitude larger than that in the second phase.
R: As stated in LN 386-388 (original version), the strong increasing trends for $\delta^{15}N^{SP}$ and $\delta^{18}O$ were most likely due to the unexpectedly low $\delta^{15}N^{SP}$ and $\delta^{18}O$ values in summer 2014 (Fig. 2). In addition, this has been discussed in section 4.3: "Nevertheless, our observation period is shorter than that of other studies, so the interannual trends determined here are more likely affected by year-to-year variability" (LN 540-542; original version).

15. L 438: I would suggest moving Fig. S7 onto the main text as it is the unique visualization to illustrate Lagrangian footprint of isotopic signatures of the sources.
R: Agree.

16. L 442 – 451: The section 4.1 does not seem to benefit the main theme of this manuscript. It rather makes the manuscript loose. Analytical quality has already mentioned in the section 2.4 Data analysis (see the lines 246, 252 – 253) and the excellent analytical repeatability for $\delta^{15}N^{SP}$ by QCL is well described in Mohn et al. (2014).
R: Although an excellent repeatability of singular measurements has been shown by (Mohn et al., 2014), it is important that repeated measurements of target gases show a good consistency, indicating long-term robustness of our measurements. This is crucial for isotopic measurements of background atmosphere, as target variabilities of our samples are most likely in a range that is only a few times larger than our analytical precision (Toyoda et al., 2013). Therefore, we would like to

keep this section. To avoid confusion, we have now changed "analytical repeatability" to "target repeatability".

17. L 458: Decock and Six (2013) does not describe the STE process at all. Is it an error in citation?
R: The reviewer is right. We have now revised the citation.

18. L 459: Add superscript "bulk" next 15N.
R: Superscript "bulk" is used for $\delta^{15}N$ values, which refer to the average of $\delta^{15}N^{\alpha}$ and $\delta^{15}N^{\beta}$. Here, enrichment of ^{15}N is a general description, thus not requiring "bulk" notation.

19. L 461: Comparing Figure 3(a) in Toyota et al. (2013) with Figure 1a here, it does not look "almost identical", but perhaps comparable. The monthly mixing ratio of N_2O at Jungfraujoch is at maximum in June while in April at Hateruma Island, Japan.
20. L 464: What are the underlying mechanisms?

21. L 511: Provide the regression coefficients in Figure S8.
R: They have been already embedded in each figure as red fonts.

22. L 514: $\delta^{15}N^{bulk}$ in Figure S7 is not particularly high in spite of potential influence of STE. It needs to be clarified.
R: This must be a misunderstanding. In Figure S7, we compared $\delta^{15}N^{bulk}$ for six air mass footprint clusters but not showing air coming from stratosphere.

23. L 537: Add minus sigh before 0.06.
24. L 558 – 559: Rahn and Wahlen (2000) do not provide clear evidence on the influence soil water vapor to oxygen isotope in N_2O, but they speculated. Thus, it would appropriate to write "… assuming that …" instead of "… given that …".
R: OK

25. L 605: The authors' argument is not clear here. Based on the isotopic signatures of the anthropogenic N_2O, long-term observation at Jungfraujoch indicates the significant contribution of denitrification process in soil while the results from Park et al. (2012) or Prokopiou et al. (2017) favor nitrification process in soil. This is clearly contradicted each other.
R: Based on the difference between our and other studies in box-model estimates, we suggest that the isotopic signatures of anthropogenic sources may have shifted in recent decades. This would mean non-linear change of N_2O source isotopic signatures since preindustrial times. On the other hand, the uncertainty in measuring N_2O isotopic signatures in the background atmosphere and inter-comparability among laboratories may play a role in the discrepancy of the estimated source isotopic signatures. Further elaborations are incorporated now (section 4.4).

26. L 617: Figure 6 shows that $\delta^{15}N^{bulk}$ from Jungfraujoch are higher than any other values including Park et al. (2012) and even Toyota et al. (2013). Thus, this sentence does not help explain why $\delta^{15}N^{bulk}$ of the anthropogenic N_2O from the observation at Jungfraujoch is higher than the value by Park et al. (2012).

27. L 618: It is impossible to mention trends of $\delta^{15}N^{SP}$ as the data is too scattered. In addition, $\delta^{15}N^{SP}$ at Jungfraujoch shows positive trends, too (Table 1).
R: Thank you for the critical comments. We have now clarified these two points in the discussion. Below are some explanations.
The difference in $\delta^{15}N^{bulk}$ between our study and Toyoda et al. (2013) is relatively small (0.10-0.15‰ based on year-to-year comparison) compared with the difference between ours and Park et al. (2012) (0.40-0.5‰). Therefore, the $\delta^{15}N^{bulk}$ of anthropogenic source estimated with two-box model is much smaller in Park et al. (2012) than in ours and Toyoda et al. (2013). Even larger inter-laboratory differences in $\delta^{15}N^{bulk}$ have been observed in Ostrom et al. (2018) and can be explained by different anchoring to international scales (Air-N2).
As stated in section 4.4, the difference between current mean tropospheric isotopic values and preindustrial values (given in Table S1) are important in determining the trend of N_2O isotopic signatures in the model estimates. The trends mentioned here are referred to long-term trends since preindustrial times as simulated by the model, but not the observed trends in the "current" troposphere.

28. L 652: What do the authors mean the "higher-frequency temporal variation" for $\delta^{15}N^{SP}$ and $\delta^{18}O$? Is it relevant to soil emission? Please state it clearly.
R: This is not referred to soil emissions. The determined interannual trends for $\delta^{15}N^{SP}$ and $\delta^{18}O$ showed large uncertainties, which is possibly due to large temporal (seasonal) variabilities of $\delta^{15}N^{SP}$ and $\delta^{18}O$. We have reformulated this statement.

29. L 656: Table 2 clearly shows the isotope signatures from Jungfraujoch differ from the values obtained at other sites, opposite to the statement here.
R: Within model uncertainty, our model estimates of isotopic signatures for anthropogenic sources were largely in agreement with the other studies, except for the $\delta^{15}N^{bulk}$ and $\delta^{15}N^{SP}$ when compared with Park et al. (2012) and Prokopiou et al. (2017).

List of all relevant changes (referred to Line numbers in the version with marked changes):

Line 52: "Tian et al., 2018" changed to "Tian et al., 2019".

Line 173-177: Add description of N_2O mixing ratio measurements at Junfraujoch: "Measurements of N_2O mixing ratios at Jungfraujoch were calibrated with three standard gases (319, 327 and 342 ppb) and accompanied with measurement of a working standard (331 ppb) every 160 minutes to account for instrumental drift. In addition, daily short (two times every 40 hours) and long-term (every 40 hours) target measurements were included to monitor the data quality".

Line 186-188: Add "Details on measurement methods and calibration strategies can be found in Zellweger et al. (2009) for CO, Pandey Deolal et al. (2012) for NO_y and Logan et al. (2012) for O_3".

Line 240: Add descriptions of CG1 and CG2 (in 78% N_2 and 21% O_2).

Line 356: "for the second half of the study" is corrected as "after the first year (2015-2018)".

Line 363-367: Reformulated discussion of difference in N_2O growth rates between the first and other years' measurements: "This difference in N_2O growth rates is probably due to the limited data quality of GC-ECD, although a lower growth rate in 2014 compared to 2015-2018 cannot be excluded. It is noteworthy that the N_2O growth rate determined for 2015 to 2019 at Jungfraujoch is slightly above the global mean growth rate for the recent decade reported by NOAA (0.93 ± 0.03 nmol mol^{-1} a^{-1}) (WMO, 2018).".

Line 432-434: Add explanation of O_3 maxima in late spring to summer: "The late spring-to-summer maxima for O_3 mixing ratios may be attributed to air mixing with stratosphere and/or planetary boundary layer, similar to the findings from a previous study at Jungfraujoch (Tarasova et al., 2009).".

Line 470-472: Supporting evidence of mixing with stratospheric air in late summer at Jungfraujoch: "This is supported by a FLEXPART model simulation of the contribution of upper tropospheric air to Jungfraujoch station, showing highest contributions in August (Fig. S7; Henne et al., Personal Communication).".

Line 502-508: Revised discussion of how soil emission can outcompete STE in regulating seasonal variability of $\delta^{15}N^{SP}$-N_2O: "Previous field studies have demonstrated that low- $\delta^{15}N^{SP}$ N_2O emissions, i.e. following the denitrification pathway, predominates during summer periods at Swiss (Wolf et al., 2015) and German (Ibraim et al., 2019) grasslands. On the other hand, the STE process is likely to exert a much smaller isotopic effect on the tropospheric N_2O (Toyoda et al., 2018). By estimating the contributions of two processes to N_2O enhancement/depletion in the late summer, we calculated the combined isotopic effects of both processes (see more details in the supplementary material), indicating that the negative effect of soil N_2O emission on $\delta^{15}N^{SP}$ likely outcompetes the positive effect by STE.".

Line 533-539: Add explanation of inconsistent trend of $\delta^{15}N^{SP}$ in the second phase: "For example, in the second phase, we detected only a significant seasonality of $\delta^{15}N^{SP}$, with a minimum in July, which is one month earlier than the summer minimum found for the whole dataset (Fig. 3). This may be attributed to a difference in source regions, as that Northwest regions appeared to be

significantly more important during 2017 (second phase). However, due to low sampling frequency, it is challenging to overcome the large uncertainty in seasonality analysis for a two-year period such as the second phase.".

Line 605-608: Describe the box-model run with dataset filtered for free troposphere: "The model runs with the whole dataset (Table 2) and the dataset filtered for free-troposphere only (Table S3) exhibit statistically identical results, supporting that our model estimates, with observations at Jungfraujoch, are representative of the background atmosphere."

Line 631-636: Discussion on the difference between this study and Park et al. (2012) in the simulated trends of $\delta^{15}N^{SP}$-N_2O by two-box model: "This may suggest that a strong climate change feedback has recently resulted in significant shifts in N_2O source process, hence twisting the isotopic signatures of anthropogenic sources (Griffis et al., 2017; Xu-Ri et al., 2012). Alternatively, the uncertainty in determining N_2O isotopic signatures in the background atmosphere and inter-laboratory comparability may play a role in the observed discrepancy."

Line 644-649: Further explanation of how mean levels of $\delta^{15}N^{SP}$- and $\delta^{15}N^{SP}$-N_2O affect the box-model results: "For example, given the similar parameters used for preindustrial times as our study, Park et al. (2012) observed much lower $\delta^{15}N^{bulk}$ in the recent troposphere than in our case, hence resulting in significantly lower $\delta^{15}N^{bulk}$ for the anthropogenic source. Furthermore, Park et al. (2012) and Prokopiou et al. (2017) simulated a positive trend in $\delta^{15}N^{SP}$ relative to preindustrial times, which in return resulted in a much higher $\delta^{15}N^{SP}$ for the anthropogenic sources.".

Figure 5: Newly added from Figure S7 in SI.

The isotopic composition of atmospheric nitrous oxide observed at the high-altitude research station Jungfraujoch, Switzerland

Longfei Yu[1*], Eliza Harris[1†], Stephan Henne[1], Sarah Eggleston[1], Martin Steinbacher[1], Lukas Emmenegger[1], Christoph Zellweger[1] and Joachim Mohn[1]

[1]Laboratory for Air Pollution & Environmental Technology, Empa, Swiss Federal Laboratories for Materials Science and Technology, Ueberlandstr. 129, CH-8600 Duebendorf, Switzerland.

[†]Current address: Institute of Ecology, University of Innsbruck, Sternwartestrasse 15, A-6020 Innsbruck, Austria

[*] Correspondence: L. Yu (longfei.yu@empa.ch)

Abstract

Atmospheric nitrous oxide (N_2O) levels have been continuously growing since preindustrial times. Mitigation requires information about sources and sinks on the regional and global scales. Isotopic composition of N_2O in the atmosphere could contribute valuable constraints. However, isotopic records of N_2O in the unpolluted atmosphere remain too scarce for large-scale N_2O models. Here, we report the results of discrete air samples collected weekly to bi-weekly over a five-year period at the high-altitude research station Jungfraujoch, located in central Switzerland. High-precision N_2O isotopic measurements were made using a recently developed preconcentration-laser spectroscopy technique. The measurements of discrete samples were accompanied by *in situ* continuous measurements of N_2O mixing ratios. Our results indicate a pronounced seasonal pattern with minimum N_2O mixing ratios in late summer, associated with a maximum in $\delta^{15}N^{bulk}$ and a minimum in intramolecular ^{15}N site preference ($\delta^{15}N^{SP}$). This pattern is most likely due to stratosphere-troposphere exchange (STE), which delivers N_2O-depleted but ^{15}N-enriched air from the stratosphere into the troposphere. Variability in $\delta^{15}N^{SP}$ induced by changes in STE may be masked by biogeochemical N_2O production processes in late summer, which are possibly dominated by a low-$\delta^{15}N^{SP}$ pathway of N_2O production (denitrification), providing an explanation for the observed seasonality of $\delta^{15}N^{SP}$. Footprint analyses and atmospheric transport simulations of N_2O for Jungfraujoch suggest that regional emissions from the planetary boundary layer contribute to seasonal variations of atmospheric N_2O isotopic composition at Jungfraujoch, albeit more clearly for $\delta^{15}N^{SP}$ and $\delta^{18}O$ than for $\delta^{15}N^{bulk}$. With the time-series of five years, we obtained a significant interannual trend for $\delta^{15}N^{bulk}$ after deseasonalization (-0.052±0.012‰ a^{-1}), indicating that the atmospheric N_2O increase is due to isotopically depleted N_2O sources. We estimated the average isotopic signature of anthropogenic N_2O sources with a two-box model to be -8.6±0.6‰

for $\delta^{15}N^{bulk}$, 34.8±3‰ for $\delta^{18}O$ and 10.7±4‰ for $\delta^{15}N^{SP}$. Our study demonstrates that seasonal variation of N_2O isotopic composition in the background atmosphere is important when determining interannual trends. More frequent, high-precision and inter-laboratory compatible measurements of atmospheric N_2O isotopocules, especially for $\delta^{15}N^{SP}$, are needed to better constrain anthropogenic N_2O sources, and thus the contribution of biogeochemical processes to N_2O growth on the global scale.

1 Introduction

Nitrous oxide (N_2O) is a potent greenhouse gas (Fowler et al., 2015) and a strong stratospheric ozone-depleting substance (Ravishankara et al., 2009). For several decades, near-surface atmospheric N_2O mixing ratios have been continuously measured at a series of remote sites, within the networks of the Global Atmosphere Watch Programme (JMA and WMO, 2018), the Advanced Global Atmospheric Gases Experiment (AGAGE) (Prinn et al., 2018), and the National Oceanic and Atmospheric Administration (NOAA) Earth System Research Laboratory (ESRL) Global Monitoring Division (GMD) (Nevison et al., 2011). These measurements have shown a significant increase in atmospheric N_2O mixing ratio, at a current growth rate of about 0.93 nmol mol^{-1} a^{-1} (WMO, 2018). On the global scale, given excessive nitrogen (N) fertilizer application, agriculture is known to be the largest and most important anthropogenic source of N_2O (Reay et al., 2012; Tian et al., ~~2018~~2019). However, long-term observations of N_2O in the unpolluted atmosphere have shown seasonal and interannual variabilities as well as interhemispheric differences in N_2O mixing ratios (Nevison et al., 2011; Thompson et al., 2014a, 2014b), which cannot yet be resolved by atmospheric transport models and existing emission inventories. Moreover, regional contributions of N_2O emissions and the strengths of individual N_2O production pathways remain difficult to quantify.

Isotopic signatures of atmospheric N_2O can provide important constraints on N_2O sources (Denk et al., 2017) and trends (Kim and Craig, 1993). The ratios of $^{15}N/^{14}N$ and $^{18}O/^{16}O$ in N_2O are often reported in δ notation as $\delta(^{15}N/^{14}N)$ and $\delta(^{18}O/^{16}O)$, abbreviated as $\delta^{15}N^{bulk}$ (average for $^{14}N^{15}N^{16}O$ and $^{15}N^{14}N^{16}O$) and $\delta^{18}O$, respectively. A large fraction of N_2O emitted to the atmosphere originates from soil bacterial processes, which usually emit N_2O that is more enriched in light (^{14}N, ^{16}O) isotopes than the tropospheric background (Pérez et al., 2001; Snider et al., 2015a; Toyoda et

al., 2017). By contrast, N_2O produced in the oceans (Bourbonnais et al., 2017; Fujii et al., 2013) and emitted from fossil fuel combustion (Ogawa and Yoshida, 2005; Toyoda et al., 2008) has higher $\delta^{15}N^{bulk}$ and $\delta^{18}O$ values which are comparable to the tropospheric background. A recent study has summarized isotopic signatures of anthropogenic N_2O sources divided into the EDGAR (Emissions Database for Global Atmospheric Research) emission categories (Janssens-Maenhout et al., 2019), showing differences in isotopic signatures between agricultural ($\delta^{15}N^{bulk}$ = -17.8 to -1.0‰ and $\delta^{18}O$ = 23.9 to 29‰) and industrial sources ($\delta^{15}N^{bulk}$ = -28.7 to 5.5‰ and $\delta^{18}O$ = 28.6 to 40.3‰) (Harris et al., 2017). These empirical ranges, together with isotopic mixing models, provide a valuable approach to interpret variability in atmospheric N_2O mixing ratios.

A number of studies have analyzed temporal trends in N_2O isotopic composition in the modern atmosphere (Kaiser et al., 2003; Park et al., 2012; Röckmann and Levin, 2005; Toyoda et al., 2013) and in the past from firn and ice cores (Bernard et al., 2006; Ishijima et al., 2007; Prokopiou et al., 2018; Röckmann et al., 2003; Sowers et al., 2002). These isotopic measurements have shown a decrease in both $\delta^{15}N^{bulk}$- and $\delta^{18}O$-N_2O associated with an increasing trend in atmospheric N_2O mixing ratios since preindustrial times, indicating that the recent increase of atmospheric N_2O may be due to agricultural emissions (^{15}N and ^{18}O depleted). The reported trend since the 1960s seems rather steady (-0.034±0.005 ‰ a^{-1} for $\delta^{15}N^{bulk}$ and -0.016 ‰±0.006 a^{-1} for $\delta^{18}O$) (Bernard et al., 2006; Ishijima et al., 2007; Park et al., 2012; Prokopiou et al., 2017; Röckmann et al., 2003; Röckmann and Levin, 2005). However, a more recent (1999-2010) study reported a smaller decreasing trend in $\delta^{15}N^{bulk}$ and only an insignificant trend in $\delta^{18}O$ for the Northern Hemisphere (Toyoda et al., 2013). Several hypotheses were proposed to explain the differences in the observed trends: 1) the interhemispheric difference in N_2O emission sources results in inconsistent isotopic signatures among different studies (Thompson et al., 2014b); 2) uncertainties in isotopic

measurements and variable sampling schemes (air type, sampling frequency and time) mask the small secular trend of N_2O isotopic composition in the background atmosphere (Toyoda et al., 2013); and/or 3) N_2O source isotopic signatures have changed in recent years, possibly due to shifts in N fertilizer type and climatic forcing (Tian et al., 2018). Hence, further investigation into the global N_2O source inventory and its evolution over time requires more frequent, precise measurements of N_2O isotopocules in the unpolluted atmosphere, particularly in the Northern Hemisphere.

Recently, site-specific composition of N_2O isotopomers (site preference: $\delta^{15}N^{SP}$), which denotes the difference of ^{15}N between the central ($^{14}N^{15}N^{16}O$, α position) and terminal ($^{15}N^{14}N^{16}O$, β position) N atoms, has been applied to constrain sources contributing to atmospheric N_2O (Toyoda et al., 2013; Yoshida and Toyoda, 2000). $\delta^{15}N^{SP}$ of N_2O is particularly effective for distinguishing between the major N_2O production processes, i.e. nitrification and denitrification, generally referred to as aerobic and anaerobic N_2O production, with high and low $\delta^{15}N^{SP}$, respectively (Sutka et al., 2006). However, despite the advantages of $\delta^{15}N^{SP}$ measurements, existing long-term studies have not yet been able to reach a definitive understanding of the $\delta^{15}N^{SP}$-N_2O trend, showing both positive (Bernard et al., 2006; Park et al., 2012; Röckmann and Levin, 2005) and negative tendencies (Röckmann et al., 2003) over the last four decades. This is probably due to an insufficient analytical precision and poor inter-laboratory agreement, in particular as the aforementioned studies are all based on isotope ratio mass spectrometry (IRMS). To retrieve site-specific isotopic information by IRMS, the N_2O^+ molecular ions and the NO^+ fragment ions are analyzed and raw data have to be corrected for rearrangements of central and terminal N and ^{17}O content (Toyoda et al., 2001). Inappropriate correction algorithms and the limited availability of

reference materials (Ostrom et al., 2018) further enlarge the analytical uncertainty (Mohn et al., 2014).

Seasonal variability in atmospheric N_2O isotopic composition, which could affect the longer-term trends, is still rarely reported in the literature (Park et al., 2012; Toyoda et al., 2013). Moreover, studies of seasonality of N_2O isotopic composition are limited to the recent past since the air samples derived from firn and ice cores suffer from coarse temporal resolution (< 2 samples per year). Park et al. (2012) studied seasonality of atmospheric N_2O isotopic composition by analyzing a set of archived air samples collected from Cape Grim (Australia) using a sophisticated mathematical modeling approach. They found consistent seasonal patterns in $\delta^{15}N^{bulk}$, $\delta^{18}O$ and $\delta^{15}N^{SP}$ of atmospheric N_2O, showing highest $^{15}N/^{18}O$ enrichment in June and lowest in December. This pattern was negatively correlated with the seasonality of the N_2O mixing ratios (lowest in April-May and highest in December), which is in agreement with a previous study by Nevison et al. (2011). The negative correlation between isotopic composition and mixing ratios has been explained by stratosphere-troposphere exchange (STE), which transports N_2O-depleted but isotopically enriched stratospheric air (prevailing reduction process) into the lower atmosphere (Yung and Miller, 1997). However, in a more recent study from Hateruma Island (Japan), Toyoda et al. (2013) reported insignificant seasonal patterns in atmospheric N_2O isotopocules (smaller variability than measurement precision), despite their finding of a somewhat similar seasonal pattern in N_2O mixing ratio (minimum in July). Although there are interhemispheric differences in N_2O sources and distinct sampling frequencies in the two studies discussed above (2-3 times per year versus monthly), it is noteworthy that both studies observed significantly larger variability in $\delta^{15}N^{SP}$ than in $\delta^{15}N^{bulk}$ and $\delta^{18}O$. Whether the fluctuations in $\delta^{15}N^{SP}$ are mainly caused by the

limited repeatability of the chosen analytical techniques or interplay of processes or mechanisms regulating atmospheric N_2O remains to be tested (Park et al., 2012).

With inherent selectiveness, in particular for site-specific isotopic composition, laser spectroscopy provides a new analytical approach for direct, precise measurements of all four N_2O isotopocules (Harris et al., 2014; Mohn et al., 2012). The recent development of quantum cascade laser absorption spectroscopy (QCLAS) coupled with an automated preconcentration unit has been applied to measure N_2O isotopocules in ambient air, with comparable precision for $\delta^{15}N^{bulk}$ and $\delta^{18}O$ and superior precision for $\delta^{15}N^{SP}$ relative to IRMS systems (Harris et al., 2017; Mohn et al., 2014). Here, we present results from the application of a preconcentration unit coupled to QCLAS to measure atmospheric N_2O isotopocules in background air collected at the high altitude research station Jungfraujoch, Switzerland. Between April 2014 and December 2018, we collected weekly to bi-weekly air samples for N_2O isotopic analyses, in parallel with online measurement of N_2O mixing ratios. To our knowledge, this work reports the first time-series of background atmospheric N_2O isotopic composition using laser spectroscopy. With this unique dataset, we aim to 1) constrain seasonal patterns of three N_2O isotopic signatures at the Jungfraujoch observatory; 2) determine interannual trends in N_2O isotopocules, especially $\delta^{15}N^{SP}$; and 3) interpret the observed patterns in N_2O mixing ratios using temporal trends in N_2O isotopic composition and reported isotopic signatures of anthropogenic sources.

2 Materials and Method

2.1 Site description

The high altitude research station Jungfraujoch (3580 m above sea level), located on the northern ridge of the Swiss Alps, is a well-established site for studying unpolluted atmosphere over Central Europe (e.g. Buchmann et al., 2016). Although the station is located in the free troposphere most of the time, it is occasionally affected by air recently lifted from the planetary boundary layer (Herrmann et al., 2015; Zellweger et al., 2003). Henne et al. (2010) investigated the representativeness of 35 European monitoring stations and categorized Jungfraujoch as "mostly remote". The Jungfraujoch station is part of several national and international networks, like the meteorological SwissMetNet network operated by MeteoSwiss, the Swiss National Air Pollution Monitoring Network (NABEL), the Global Atmospheric Watch Programme (GAW) of the World Meteorological Organization (WMO) and the Integrated Carbon Observation Systems (ICOS) Research Infrastructure. This results in an extended set of long-term and continuously available parameters such as meteorological variables (Appenzeller et al., 2008), greenhouse gases (Schibig et al., 2015; Sepúlveda et al., 2014; Yuan et al., 2018), CO_2 isotopic composition (Sturm et al., 2013; Tuzson et al., 2011), ozone-depleting substances and their replacement products (Reimann et al., 2008), atmospheric pollutants (Logan et al., 2012; Pandey Deolal et al., 2012; Zellweger et al., 2009) and aerosol parameters (Bukowiecki et al., 2016).

2.2 *In situ* measurements and discrete air sampling (flasks)

In situ observations of N_2O mixing ratios commenced at Jungfraujoch in December 2004. Initially, measurements were made with gas chromatography (GC) (Agilent 6890N, USA) followed by electron capture detection (ECD). The time resolution of these measurements was 24 to 30 minutes.

In late 2014, we implemented a cavity-enhanced off-axis integrated cavity out-put spectroscopy analyzer (OA-ICOS, Los Gatos Research Inc., Mountain View, CA, USA), which measures the atmospheric N_2O mixing ratio continuously. Measurements of N_2O mixing ratios at Jungfraujoch were calibrated with three standard gases (319, 327 and 342 ppb) and accompanied with measurement of a working standard (331 ppb) every 160 minutes to account for instrumental drift. In addition, ~~daily~~ short (two times every 40 hours) and long-term (every 40 hours) –target measurements were included to monitor the data quality ~~to account for instrumental drift long terms~~. Due to the superior measurement precision compared to the GC-ECD method (Lebegue et al., 2016), the OA-ICOS record has become the primary time-series since January 2015. The GC-ECD observations continued until summer 2016 for comparison and quality control.

Additional parameters, recorded within the NABEL network and the ICOS infrastructure, were included in the analysis below. These data were carbon monoxide (CO) (measured by cavity ring-down spectroscopy; Model G2401, Picarro Inc., USA), the sum of oxidized nitrogen species (NO_y) (measured by chemiluminescence detection after conversion of NO_y to NO on a heated gold catalyst; CLD 89p, Eco Physics, Switzerland) and O_3 (measured by UV absorption; TEI 49i, Thermo Scientific, USA). Details on measurement methods and calibration strategies can be found in Zellweger et al. (2009) for CO, Pandey Deolal et al. (2012) for NO_y and Logan et al. (2012) for O_3.

In conjunction with the online measurements, we deployed an automated sampling system (Fig. S1) to collect pressurized air samples in aluminum cylinders from the same air inlet at the Sphinx observatory ~~in~~of the Junfraujoch station, for subsequent N_2O mixing ratio and isotopic analyses. The sample collection was conducted weekly from April 2014 to February 2016. After a sampling gap of five months due to a technical failure, we reinitiated a bi-weekly sampling, which continued

194 from August 2016 to December 2018. The sampling system, automated by a customized LabVIEW
195 program (National Instruments Corp., USA), consisted of a Nafion drier (PD-100T-48MSS, Perma
196 Pure LLC, USA), a membrane gas compressor (KNF Neuberger, USA; Type N286 series), a 16-
197 port selector valve (EMT2CSD16MWEPH, VICI AG, Swtizerland), and a rack to accommodate
198 nine 2-L aluminum flasks (Luxfer, Messer Schweiz AG, Switzerland). During sample filling, pre-
199 evacuated flasks were first purged with ambient air five times (1 hour), and then filled to 12000
200 hPa within 40 min, resulting in approximately 24 L (298 K and 1000 hPa) of air per flask for
201 isotopic analysis. Air sample filling generally took place between 2:00 and 3:00 pm local time at
202 each sampling day. Sample flasks were sent back to the laboratory at Empa for analyses every few
203 months. For this study, 142 air samples were collected in flasks and analyzed for N_2O isotopocules.

204 **2.3 Analyses of discrete air samples**

205 Discrete air samples were regularly analyzed in batches but note in chronological order to prevent
206 the imprint of analytical drifts on temporal trends of the samples. N_2O mole fractions were
207 analyzed by QCLAS (CW-QC-TILDAS-76-CS, Aerodyne Research Inc., USA) against NOAA
208 standards on the WMO-X2006A calibration scale (Hall et al., 2007), at a precision around 0.1
209 nmol mol^{-1} (determined with the average of 1-min data).

210 The four most abundant N_2O isotopocules ($^{14}N^{14}N^{16}O$, 99.03%; $^{14}N^{15}N^{16}O$, 0.36%; $^{15}N^{14}N^{16}O$,
211 0.36%; $^{14}N^{14}N^{18}O$, 0.20%) were analyzed using a customized QCLAS system (Aerodyne Research,
212 Inc., USA) (Heil et al., 2014) coupled with an automated preconcentration device (Mohn et al.,
213 2010). Before entering the pre-concentration unit, sample air is passed through a Sofnocat 423 trap
214 (Molecular Products Limited, GB) to remove CO, and subsequently through an Ascarite trap
215 (Ascarite: 6 g, 10–35 mesh, Sigma Aldrich, Switzerland, bracketed by $Mg(ClO_4)_2$, 2 × 1.5 g, Alfa
216 Aesar, Germany) to remove CO_2 and water. Approximately 5.5 L of air with a flow of 250 ml min^{-}

[1] (at 295 K and 3500 hPa) is then passed through a HayeSep D trap cooled to -145 °C to collect N_2O (Mohn et al., 2010). For N_2O release to the multipath cell of the QCLAS, the HayeSep D trap is quickly heated to 10 °C and flushed with high-purity synthetic air (20.5% of O_2 in N_2) carrier gas at a flow rate of 25 ml min^{-1} (at 295 K and 3500 hPa). A final cell pressure around 16 hPa is achieved, which results in an N_2O mixing ratio of about 45 μmol mol^{-1}. More instrumental details can be found in previous studies (Harris et al., 2017; Mohn et al., 2010, 2012). Sample tanks were each analyzed twice to yield duplicates for N_2O isotopic results, which left sufficient air for amount fraction analysis as described in the previous paragraph.

2.4 Data analyses

We used 10-minute averages of the continuous *in situ* measurements from the Jungfraujoch station across this study. For a point-to-point comparison of continuous and discrete measurements of N_2O mixing ratio, we aggregated 10-minute averages of *in situ* data for the same period when the discrete sample was filled into the cylinder (40 min).

In this study, we report abundances of N_2O isotopocules using δ notation (‰) as below:

$$\delta X = \frac{(R_{sample} - R_{standard})}{R_{standard}} \quad (1)$$

where X refers to $^{15}N^{\alpha}$ ($^{14}N^{15}N^{16}O$), $^{15}N^{\beta}$ ($^{15}N^{14}N^{16}O$) and ^{18}O ($^{14}N^{14}N^{18}O$); R refers to the ratio between the amount fractions of the rare isotopocules as mentioned above and the amount fraction of $^{14}N^{14}N^{16}O$; isotope standards refer to atmospheric N_2 for ^{15}N and Vienna Standard Mean Ocean Water (VSMOW) for ^{18}O.

Hence, the total ^{15}N content of N_2O and site-specific composition of N_2O isotopomers could be further illustrated as $\delta^{15}N^{bulk}$ and $\delta^{15}N^{SP}$, respectively, according to the equations below:

$$\delta^{15}N^{bulk} = (\delta^{15}N^{\alpha} + \delta^{15}N^{\beta})/2 \quad (2)$$

$$\delta^{15}N^{SP} = \delta^{15}N^{\alpha} - \delta^{15}N^{\beta} \quad (3)$$

Two standards (CG1, CG2; in 78% N_2 and 21% O_2) with distinct isotopic signatures ($\delta^{15}N^{\alpha}$ = 16.29 ± 0.07‰ (CG1) and -51.09 ± 0.07‰ (CG2); $\delta^{15}N^{\beta}$ = -2.59 ± 0.06‰ and -48.12 ± 0.04‰; $\delta^{18}O$ = 39.37 ± 0.04‰ and 30.81 ± 0.03‰) were used for calibrating isotopic composition. The calibration gases CG1 and CG2 were calibrated on the Tokyo Institute of Technology (TIT) scale, based on cross-calibration with primary standards assigned by TIT (Mohn et al., 2012, 2014). In addition, CG1 was measured repeatedly between samples and target gases to account for instrumental drift. Both CG1 and CG2 have N_2O mixing ratios of 45 µmol mol^{-1}, similar to the N_2O amount fraction of the samples after preconcentration. However, to correct for possible instrumental dependence on N_2O mixing ratio, CG1 was diluted to N_2O mole fractions of 35-40 µmol mol^{-1} within each measurement batch. In general, duplicated isotopic measurements of flask samples yielded values of repeatability of 0.10-0.20‰ for $\delta^{15}N^{bulk}$ and $\delta^{18}O$, and 0.15-0.25‰ for $\delta^{15}N^{SP}$.

At the beginning of the project, a batch of three cylinders (50 L water volume, Luxfer, Italy) were filled with pressurized ambient air in Dübendorf with an oil-free, three stage compressor (SA-3, Rix Industries, USA) and used as long-term target gases. The pressurized ambient air target gas was analyzed with identical treatment as Jungfraujoch air samples during every analysis batch, to monitor long-term analytical drift. Standard deviations for repeated target gas measurements throughout the period of Jungfraujoch sample measurements, were 0.13‰ for $\delta^{15}N^{bulk}$, 0.21‰ for $\delta^{15}N^{SP}$, and 0.11‰ for $\delta^{18}O$ (Fig. S2).

2.5 Surface air footprint analysis and simulated regional N_2O enhancement

We analyzed the air mass origin at Jungfraujoch by applying the Lagrangian particle dispersion model (LPDM) FLEX-PART in the backward mode (Stohl et al., 2005). The model was driven by meteorological fields taken from the ECMWF-IFS operational analysis cycle, extracted at a resolution of $1^{o}\times1^{o}$, 90/137 levels globally, and at higher horizontal resolution of $0.2^{o}\times0.2^{o}$ for central Europe. We released 50000 virtual air parcels every 3 hours at 3000 m a.s.l. from Jungfraujoch to perform backward dispersion simulations over 10 days, which allowed us to calculate surface source sensitivities (concentration footprints). A release height of 3000 m a.s.l. was previously determined to be an optimum for simulating concentration footprints at Jungfraujoch, given the stated horizontal resolution which results in a considerable smoothing of the complex, alpine orography (Keller et al., 2012). The 3-hourly surface footprints for the whole observation period were used to categorize different transport regimes using the clustering approach outlined in Sturm et al. (2013). This allowed us to distinguish among six different source regions: Free Troposphere (FT), Southwest (SW), East (E), Local (L), West (W) and Northwest (NW).

Similar to Henne et al. (2016) for CH_4 and based on spatially resolved N_2O emission inventories (Meteotest for Switzerland; EDGAR for Europe), we used the FLEXPART concentration footprints to calculate time-series of atmospheric mole fraction increases at Jungfraujoch resolved by emission sectors (Henne et al., 2016). The emission inventory by Meteotest consists of 12 emission sectors, among which all sectors except "organic soils" are comparable to sectors in the EDGAR inventory (See Table ~~S2~~S1) (Janssens-Maenhout et al., 2019). To improve seasonal representation of the emissions in our model, we used a monthly resolved, optimized version of the emission inventory, which was obtained through inverse modeling using the N_2O atmospheric mole fractions observed between March 2017 and September 2018 at the tall tower site

Beromuenster on the Swiss plateau (Henne et al., 2019). Therefore, in this study, source contributions to Jungfraujoch were estimated specifically for the period mentioned above.

2.6 Evaluation of seasonal pattern and interannual trend for time-series

To explore seasonality and interannual trends, we fit the time-series of *in situ* measurements of N_2O and O_3 mixing ratios, NO_y-to-CO ratios and isotopic measurements of N_2O with polynomial functions and Fourier series (four harmonics for *in situ* measurements and two harmonics for discrete measurements) (Thoning et al., 1989). Time-series were then decomposed into a linear trend, seasonal variability (per 12 months) and residuals. This fit was conducted with a nonlinear least-squares (NLS) model with R-3.5.3 (R Core Team, 2016). The detrended seasonality was examined by comparing peak-to-peak amplitudes with our analytical precisions and the uncertainty given by the one standard deviation of monthly residuals. To determine interannual trends, a linear regression was applied to both the raw and the deseasonalized datasets. The significance level is set to $p < 0.01$. The interannual trends for N_2O mixing ratios were found to be little affected by seasonality, so growth rates were determined only based on the raw datasets.

Although Jungfraujoch is a remote site, episodic influence from the planetary boundary layer can be observed at the station (Pandey Deolal et al., 2012; Zellweger et al., 2003). For evaluating trends of N_2O mixing ratio measurements, we filtered out *in situ* data with significant influence of plenary boundary layer, in order to represent a major air mass footprint from the free troposphere (FT). In addition to the air transport regimes, an alternative filtering criteria for the free troposphere was based on the published mean ranges of NO_y mixing ratios (501-748 ppt depending on the season) and NO_y to CO ratios (0.003-0.005 depending on the season) at Jungfraujoch (Zellweger et al., 2003). This criterion is less strict than that given by footprint analyses (Herrmann et al., 2015).

After applying this criterion to the isotopic time-series (which led to the exclusion of 32 measurement points), we re-evaluated the seasonal and interannual trends in the N_2O isotopic composition. In addition, because of the strong variability observed for isotopic data during the first 1.5 years (until February 2016), we performed an independent evaluation for the time-series starting from August 2016.

2.7 Two-box model simulation

A two-box model representing a well-mixed troposphere and stratosphere was used to estimate the anthropogenic N_2O source strength and isotopic composition from the trends measured at Jungfraujoch, similar to the approaches used by several previous studies (Ishijima et al., 2007; Röckmann et al., 2003; Schilt et al., 2014; Sowers et al., 2002). The input variables used to run the model are given in Table ~~S1~~S2. 200 iterations of the model were run using a Monte Carlo-style approach to approximate the uncertainty considering the uncertainty distribution for each input variable as given in Table ~~S1~~S2. All variables were set independently within the Monte Carlo approximation except for preindustrial N_2O life time (τ~~T~~$_{PI}$), which was fixed to 106% of the present-day N_2O life time τ~~T~~$_{PD}$ (Prather et al., 2015).

Within each iteration of the model, the preindustrial N_2O burden was first described, assuming steady state in the preindustrial era. The preindustrial stratospheric N_2O mixing ratio ($c_{S,PI}$) (270±7.5 nmol mol^{-1}) was taken from Sowers et al. (2002):

$$0 = TS_{ex}\left(c_{PI} - c_{S,PI}\right) - (M_{PI} + M_{S,PI})/\tau_{PI} \quad (4)$$

where TS_{ex} refers to the troposphere-stratosphere exchange rate; c_{PI} refers to the preindustrial tropospheric N_2O mixing ratio; and M_{PI} and $M_{S,PI}$ are the masses of N_2O in the troposphere and stratosphere respectively. The preindustrial terrestrial flux in Sowers et al. (2002) (equation 2) was

used here assuming no anthropogenic emissions. The delta values for the preindustrial stratosphere and the fractionation factor for the stratospheric sink were taken from equations 6 and 7 from Sowers et al. (2002) assuming steady state and no anthropogenic emissions. The model was run with a yearly time step starting from the preindustrial assuming that anthropogenic emissions began in 1845 (Sowers et al., 2002). For each year of the model run, the anthropogenic flux was calculated according to the exponential increase described by Sowers et al. (2002):

$$F_{\text{anth},t} = e^{\alpha(t-t_0)} - 1 \quad (5)$$

where t is the current year, t_0 = 1845 and α is the growth rate (assumed to be constant). The rates of change for tropospheric and stratospheric N_2O mixing ratios were then retrieved from equations 2 and 3 in Sowers et al. (2002), and for the isotopic composition of stratospheric and tropospheric N_2O from equations 6 and 7 in Sowers et al. (2002).

The values of the parameters describing the anthropogenic flux were optimized to fit both the trend and the absolute values for the five years of Jungfraujoch isotope data, and the mixing ratio data from the Jungfraujoch flasks and *in situ* data since 2005 (GAW data source). The uncertainties in α and in the anthropogenic source isotopic signatures were approximated by one standard deviation of values derived from repeated model runs.

2.8 "Bottom-up" estimates of source isotopic signatures

To gauge the accuracy of the two-box model, we deployed a "bottom-up" approach as an alternative method of estimating the N_2O source signatures. The isotopic signatures of most N_2O source sectors given in the Meteotest/EDGAR emission inventory are available from the literature, except for the "Refinery" (Table ~~S2~~S1). As "Refinery" generally contributes only about 0.02% of the N_2O emission at Jungfraujoch, it was excluded for source isotopic signature estimation. The

simulated N_2O emissions by variable sources were categorized according to the EDGAR emission types (Janssens-Maenhout et al., 2019). We then calculated isotopic signatures for the overall source and the anthropogenic sources alone (excluding indirect natural emission) as weighted averages.

3 Results

3.1 Atmospheric N_2O mixing ratios at Jungfraujoch

We observed a linear growth of atmospheric N_2O at Jungfraujoch during the period 2014-2018 (Fig. 1a). A point-to-point comparison of discrete and *in situ* measurements showed good agreement, in particular ~~for the second half of the study~~after the first year (~~2016~~2015-2018), where the data quality of *in situ* measurements was largely improved due to the implementation of the more precise laser spectroscopy method as compared to GC-ECD (Fig. S3). The improvement in analytical precision for N_2O mixing ratio was due to better temporal coverage by the OA-ICOS instrument, in contrast with the GC analyses which conduct one measurement per 24-30 minutes. The annual growth rates from 2014 to 2018 determined with *in situ* measurements were 0.880 ± 0.001 and 0.993 ± 0.001 nmol mol^{-1} a^{-1} with and without GC-ECD measurements in 2014, respectively. ~~Such~~This difference in N_2O growth rates is probably due to the limited data quality of GC-ECD, although a lower growth rate in 2014 compared to 2015-2018 cannot be excluded~~due to switch of analytical method suggests that analytical uncertainty in N_2O mixing ratios can significantly influence its linear trends.~~ It is noteworthy that the N_2O growth~~These~~ rate~~s~~ determined for 2015 to 2019 at Jungfraujoch is slightly above ~~are in agreement with~~ the global mean growth rate for the recent decade reported by NOAA (0.93 ± 0.03 nmol mol^{-1} a^{-1}) (WMO, 2018). If we filter the *in situ* dataset to examine only the "free troposphere" periods, we obtain a lower increase (0.858±0.002 nmol mol^{-1} a^{-1}). By comparison, the absolute ~~annual~~ growth rate determined from the discrete gas samples was even lower albeit larger uncertainty (0.813 ± 0.027 nmol mol^{-1} a^{-1}).

A significant seasonal pattern was observed for N_2O mixing ratios measured *in situ*, with a maximum in early summer and a minimum in late summer (Fig. 1b). For discrete N_2O

375 measurements a similar trend was observed, but the detrended seasonality was not significant,
376 which might be due to the much lower number of samples (Fig. S4).

377 **3.2 Interannual trends of N_2O isotopic composition and anthropogenic source signatures**

378 Time-series of $\delta^{15}N^{bulk}$, $\delta^{15}N^{SP}$ and $\delta^{18}O$ for atmospheric N_2O at Jungfraujoch are shown in Figure
379 2. The NLS model simulation accounts well for the variabilities of isotopic time-series. Interannual
380 trends of three isotopic deltas were determined for both raw and deseasonalized datasets by linear
381 regression (Table 1). The deseasonalized interannual trends were slightly smaller than the trends
382 determined with the raw datasets. For the whole dataset, the deseasonlized trend indicates a
383 significant decrease in $\delta^{15}N^{bulk}$, of -0.052±0.012‰ a^{-1}. In contrast, deseasonlized time-series of
384 $\delta^{15}N^{SP}$ and $\delta^{18}O$ increased, albeit insignificantly, by 0.065±0.027 ‰ a^{-1} and 0.019±0.011 ‰ a^{-1},
385 respectively. The trends determined for periods with major air mass footprints from the free
386 troposphere were close to those calculated for the whole dataset, except that $\delta^{15}N^{SP}$ trends
387 decreased after filtering out the samples with significant impact from plenary boundary layer. This
388 indicates that N_2O interannual trends observed at Jungfraujoch are of regional relevance, despite
389 the fact that a small impact from local sources can be seen. Because of the observed irregular
390 variability and the change in sampling frequency (though no change in daily sampling time) in our
391 dataset, we separated the time-series into two phases: April 2014-February 2016 (first phase;
392 weekly sampling) and August 2016-December 2018 (second phase; bi-weekly sampling). In the
393 first phase, the rates of increase in $\delta^{15}N^{SP}$ and $\delta^{18}O$ were almost one order of magnitude larger than
394 over the whole dataset. This is most likely due to the unexpectedly low $\delta^{15}N^{SP}$ and $\delta^{18}O$ in summer
395 2014 followed by a distinct increase in winter 2014-2015, which results in large rates of increase
396 over short periods. Such growth rates were not seen in the second phase, when both $\delta^{15}N^{SP}$ and

$\delta^{18}O$ showed small and insignificant variations. $\delta^{15}N^{bulk}$ displayed a decreasing interannual trend in both phases; however, the rate of decrease was larger in the second phase (-0.130±0.045‰ a^{-1}).

We tuned our two-box model to best match the observed N_2O mixing ratios and isotopic composition at Jungfraujoch. An estimate of anthropogenic emissions and source signatures is given in Table 2. For 2018, annual N_2O emissions were estimated to be 8.6±0.6 Tg N_2O-N a^{-1}. The average isotopic signatures for anthropogenic sources were -8.6±4‰, 34.8±3‰ and 10.7±4‰ for $\delta^{15}N^{bulk}$, $\delta^{15}N^{SP}$ and $\delta^{18}O$, respectively, which are clearly lower than those for preindustrial N_2O in the tropospheric background (Table ~~S1~~S2; Toyoda et al., 2013).

3.3 Seasonal variation of N_2O isotopic composition

$\delta^{15}N^{SP}$ of N_2O showed the most pronounced variability among all isotopic time-series (Fig. 2), spanning 2.5‰ for individual flask sample measurements. Seasonal variability was estimated with the NLS model and presented as mean seasonal cycles (Fig. 3). For $\delta^{15}N^{SP}$ a "summer minimum" was found regardless of whether the entire dataset or only the second phase was considered (Fig. 3), although seasonal variability of the second time-series was smaller and showed the minimum occurring earlier. The seasonal pattern of $\delta^{15}N^{bulk}$ determined from the whole dataset indicates a significant summer maximum, but this was not seen when only the data from the second phase was taken, as there was no significant seasonal pattern over this period alone. For $\delta^{18}O$, we observed only small temporal variability and a lack of seasonal pattern. In addition, seasonal variations of time-series filtered for free troposphere were evaluated; these show temporal patterns similar to the whole dataset (Fig. S5).

3.4 Air mass origin and *in situ* measurements at Jungfraujoch

Back-trajectory simulations indicate six major transport clusters during 2014-2018, as shown in Figure 4a. Four of these transport regimes (SW, E, L and NW) dominate, accounting for about 60-90% coverage of the whole period. By contrast, the free troposphere cluster only represents 10-20% of the data. Averaged monthly contributions of transport clusters are shown in Figure 4b, with more pronounced impact by the L, E and NW regions in summer and stronger contribution by FT and SW in winter. The source patterns of the air masses at Jungfraujoch were generally consistent across the years in the present study. However, an apparent discrepancy was found for discrete sampling times in the last two years (e.g. particularly low contribution from SW) which is most likely due to the low and variable sampling frequency of the discrete sample collection (Fig. 4b).

The detrended seasonal variability of *in situ* measurements indicates summer maxima for ~~O_3 and~~ NO_y mixing ratios as well as NO_y-to-CO ratios at Jungfraujoch (Fig. S6). This likely indicates stronger exchange with the polluted planetary boundary layer in summer (Herrmann et al., 2015; Zellweger et al., 2003)~~(Tarasova et al., 2009)~~, which is consistent with the seasonal pattern of air mass footprint derived from back-trajectory simulations. The late spring-to-summer maxima for O_3 mixing ratios may be attributed to air mixing with stratosphere and/or planetary boundary layer, similar to the findings from a previous study at Jungfraujoch (Tarasova et al., 2009). On the other hand, CO shows a maximum in early spring and decreases in summer when its atmospheric lifetime is shortest. Atmospheric O_3, NO_y and CO measurements during our discrete sampling periods also well represented seasonal variability shown for *in situ* measurements, except for 2016-2017 where there was a five-month sampling gap (Fig. S6).

Comparisons of air mass footprints as well as O_3, NO_y and CO mixing ratios between *in situ* and discrete sampling indicate that the discrete sampling covers the main air source regions and

441 variabilities in local pollution/free troposphere fairly well (Fig. 4 and S6). In the second phase
442 (2016-2018), the less frequent sampling impedes evaluation of the seasonal and interannual
443 variabilities.

444 **3.5 Relationship between N_2O isotopic signatures and air mass footprints**

445 We categorized N_2O mixing ratio and isotopic signature time-series into subsets based on the six
446 air mass transport clusters. One-way ANOVA among clusters indicates that N_2O mixing ratios in
447 air masses originating from cluster L were significantly higher and those from clusters FT and W
448 were significantly lower than the others (Fig. ~~S7~~5). In accordance with the pattern found for mixing
449 ratios, $\delta^{15}N^{SP}$ and $\delta^{18}O$ were high for cluster FT, and low for cluster L. For $\delta^{15}N^{bulk}$, little difference
450 between transport clusters was detected.

4 Discussion

4.1 Quality assurance of isotopic measurements

This study reports the first results of background N_2O isotopic measurements based on a laser spectroscopic technique. Benefiting from the preconcentration process, we achieved measurement repeatability for a target gas of 0.10-0.20‰ for $\delta^{15}N^{bulk}$ and $\delta^{18}O$ (Fig. S2), which is comparable to that of IRMS measurements of ambient atmosphere (Park et al., 2012; Prokopiou et al., 2017; Röckmann et al., 2003; Toyoda et al., 2013). The long-term robustness of our technique is adequate for disentangling both seasonal and interannual temporal variability as shown in Figure 2. In particular, our ~~analytical~~ repeatability of target measurements for $\delta^{15}N^{SP}$ (0.15-0.25‰) appears to be better than previous studies measuring background atmosphere or firn air (0.8‰, Park et al., 2012; 0.3‰, Prokopiou et al., 2017; 0.3‰, Toyoda et al., 2013).

4.2 Seasonal variabilities of atmospheric N_2O isotopic composition

In situ measurements of N_2O mixing ratios showed a clear early summer maximum and late summer minimum (Fig. 1). Such a seasonal pattern was previously found for a number of NOAA and AGAGE sites analyzing long-term N_2O records in the NH (Jiang et al., 2007; Nevison et al., 2011). One explanation of the late-summer minimum is a strong influence of the STE process in this period, which transports N_2O-depleted but isotopically enriched air downward from the stratosphere into the troposphere (~~Decock and Six, 2013~~Park et al., 2012; Snider et al., 2015b). During the late summer at Jungfraujoch, we find strong enrichment of ^{15}N in atmospheric N_2O according to the detrended seasonality for the whole dataset (Fig. 3). This is supported by a FLEXPART model simulation of the contribution of upper tropospheric air to Jungfraujoch station, showing highest contributions in August (Fig. S7; Henne et al., Personal Communication). At

Hateruma Island, Japan, Toyoda et al. (2013) observed a seasonal pattern of atmospheric N_2O mixing ratios almost identical to our study, but found insignificant variations of isotopic composition. On the other hand, N_2O seasonal variability could be influenced by oceanic emission sources (Jiang et al., 2007; Nevison et al., 2005), complicating the underlying mechanisms for the observed patterns. For example, in another study looking at archived air from Cape Grim, Australia, Park et al. (2012) detected an April-May minimum and a November-December maximum for N_2O. This is expected for the SH, as STE is most prevalent in April (Nevison et al., 2011). They observed negative correlations of $\delta^{15}N^{bulk}$, $\delta^{15}N^{\alpha}$ and $\delta^{18}O$ with N_2O mixing ratios, appearing to support the idea that the STE process is responsible for seasonal variabilities in N_2O mixing ratios and isotopic composition at Cape Grim. However, the seasonal cycle for $\delta^{15}N^{\alpha}$ was much larger than $\delta^{15}N^{bulk}$ and $\delta^{18}O$, which could not be explained by STE alone. They suggested that the seasonal patterns of N_2O isotopes at Cape Grim may be due to mixing between oceanic sources (high N_2O with low ^{15}N and ^{18}O) and STE (low N_2O with high ^{15}N and ^{18}O) (Nevison et al., 2011; Park et al., 2012). However, because we observe a concurrent minimum of $\delta^{15}N^{SP}$ and maximum of $\delta^{15}N^{bulk}$ in July-August with low N_2O at Jungfraujoch (Fig. 3), additional mechanisms must be considered here.

Regional model simulations based on Swiss N_2O emissions derived from the inverse method were used to explore contributions from different sources to the variability in N_2O enhancements at Jungfraujoch. As shown in Figure 5a&b, soil emissions, including direct and indirect emissions from agricultural lands and emissions from (semi-)natural areas, account for more than 70% of the total N_2O enhancements, while manure and waste management contribute another 20%. Total N_2O enhancements appeared to be highest in May to July (Fig. ~~5e~~6c), in accordance with the highest contribution by soil emissions. The early-to-middle summer maximum in the simulated N_2O enhancements is comparable with maximum of N_2O mixing ratios in early summer as observed at

Jungfraujoch (Fig. 1b). This underlines the importance of soil emission in accounting for atmospheric N_2O variability (Saikawa et al., 2014). Soil N_2O emissions are mainly derived from denitrification and nitrification, which prevail in anaerobic and aerobic soil environment, respectively (Butterbach-Bahl et al., 2013). Denitrification-derived N_2O is expected to be about 30‰ lower in $\delta^{15}N^{SP}$ than N_2O produced by nitrification (Sutka et al., 2006). Previous field studies ~~at Swiss grasslands~~ have demonstrated that low- $\delta^{15}N^{SP}$ N_2O emissions, i.e. following the denitrification pathway, ~~dominates peak N_2O fluxes observed in summer periods~~predominates during summer periods at Swiss (Wolf et al., 2015) and German (Ibraim et al., 2019) grasslands ~~(Ibraim et al., 2019)~~. On the other hand, the STE process is likely to exert a much smaller isotopic effect on the tropospheric N_2O (Toyoda et al., 2018). By estimating the contributions of two processes to N_2O enhancement/depletion in the late summer, we calculated the combined isotopic effects of both processes (see more details in the supplementary material), indicating that the negative effect of soil N_2O emission on $\delta^{15}N^{SP}$ likely outcompetes the positive effect by STE. ~~Therefore, we hypothesize that the observed minimum of $\delta^{15}N^{SP}$ in late summer at Jungfraujoch is largely contributed by the prevailing N_2O production by denitrification.~~ By contrast, the influence of biogeochemical processes (nitrification and denitrification) on $\delta^{15}N^{bulk}$ is generally smaller than that on $\delta^{15}N^{SP}$ (Toyoda et al., 2011), and such effect on $\delta^{15}N^{bulk}$ are usually overwritten by the wide range of isotopic signatures in soil N substrates (Sutka et al., 2006). Hence, given the distinct $\delta^{15}N^{bulk}$ maximum and N_2O minimum in late summer during our observation (Figs. 1 and 3), we suggest that the STE process is mainly responsible for the seasonal variability in $\delta^{15}N^{bulk}$.

The footprint analyses based on air mass residence time revealed a seasonal pattern, with a higher contribution of background air from the FT and SW regions in winter and more pronounced contribution of local planetary boundary layer air from the L, E and NW regions in summer (Fig.

519 4b). The higher frequency of air mass footprints recently in contact with the surface in summer is
520 consistent with inverse modeling results, indicating a larger contribution of soil N_2O emissions in
521 June/July (Fig. ~~5~~6). For the air mass regime representing the free troposphere, N_2O mixing ratios
522 observed at Jungfraujoch were significantly below the average, while $\delta^{15}N^{SP}$ and $\delta^{18}O$ were higher
523 (Fig. 5~~S7~~). By contrast, the local cluster (L) representing a strong impact from the planetary
524 boundary layer had higher N_2O mixing ratios and lower isotopic signatures (except $\delta^{15}N^{bulk}$) than
525 the other source regions. In addition, the ratios of NO_y to CO, which is a more ~~straight-~~
526 ~~forward~~straightforward indicator of the free troposphere (Zellweger et al., 2003), show significant
527 negative correlations with $\delta^{15}N^{SP}$ and $\delta^{18}O$, but not with $\delta^{15}N^{bulk}$ (Fig. S8). This further suggests
528 that the seasonal variability of $\delta^{15}N^{SP}$ and $\delta^{18}O$ observed at Jungfraujoch is most likely influenced
529 by ground-derived emissions, while fluctuations in N_2O mixing ratios and $\delta^{15}N^{bulk}$ are possibly
530 driven by STE.

531 Considering the complexity in mechanisms responsible for N_2O isotopic variations, we strongly
532 recommend more field measurements of N_2O isotopic signatures at higher frequency and at
533 different background sites, in order to cover spatial and temporal variability in N_2O sources. For
534 example, in the second phase, we detected only a significant seasonality of $\delta^{15}N^{SP}$, with a minimum
535 in July, which is one month earlier than the summer minimum found for the whole dataset (Fig.
536 3). This may be attributed to a difference in source regions, as ~~that~~ Northwest regions appeared to
537 be significantly more important during 2017 (second phase). However, due to low sampling
538 frequency, it is challenging to overcome the large uncertainty in seasonality analysis for a two-
539 year period such as the second phase. ~~Also, the uncertainty in seasonal patterns could be further~~
540 ~~reduced by longer and more frequent isotopic measurements – *in situ* monitoring at background~~
541 ~~sites like Jungfraujoch could be especially useful.~~

Based on our bottom-up approach, we simulated isotopic signatures for the overall N_2O sources responsible for the N_2O mixing ratio increase in the atmosphere (Fig. S9). However, the interpretation of simulated versus observed variability in N_2O isotopic composition was difficult, except for the somewhat similar patterns in $\delta^{18}O$. Our results suggest a limitation in the current knowledge and literature values on isotopic signatures of most N_2O sources. In addition, most N_2O sources may not exhibit a well-defined isotopic signature but a range of values regulated under a number of processes/environmental factors. For example, isotopic signatures of soil-derived N_2O are often determined by an interaction of several soil and climatic factors. It might be possible in the future to model these changes implementing isotopes in ecosystem models, as recently demonstrated by Denk et al. (2019).

4.3 Interannual trends of atmospheric N_2O isotopic composition

Over a period of almost five years, our observations show an interannual increase in N_2O mixing ratio and decrease in $\delta^{15}N^{bulk}$ (Fig. ~~6~~7). This is to be expected, assuming that the atmospheric N_2O increase is primarily attributed to anthropogenic sources, which emit isotopically lighter N_2O relative to the tropospheric background (Table ~~S2~~S1) (Rahn and Wahlen, 2000). Compared to several studies on firn air (Ishijima et al., 2007; Röckmann et al., 2003) and surface air (Park et al., 2012; Röckmann and Levin, 2005; Toyoda et al., 2013), the rate of decrease for $\delta^{15}N^{bulk}$ at Jungfraujoch is relatively high (-0.05 to -0.06 ‰ a^{-1}, Table 1). Such a discrepancy in the $\delta^{15}N^{bulk}$ trend could be due to a large contribution of terrestrial N_2O emission from the European continent to Jungfraujoch (Figs. 1 and 5), as N_2O originating from soil emissions is significantly more isotopically depleted than that of oceanic sources (Snider et al., 2015b). Nevertheless, our observation period is shorter than that of other studies, so the interannual trends determined here are more likely affected by year-to-year variability. Among all reported records, the decrease of

565 $\delta^{15}N^{bulk}$ observed at Hateruma Island was the most up-to-date and smallest (-0.020-0.026‰ a^{-1})
566 (Toyoda et al., 2013). The authors argued that the smaller declining trend for $\delta^{15}N^{bulk}$ may be
567 explained by the recent increase in anthropogenic isotopic ratios particularly for agricultural N_2O
568 emissions, although Ishijima et al. (2007) suggested a decline in both $\delta^{15}N^{bulk}$ and $\delta^{18}O$ in
569 anthropogenic N_2O from 1952-1970 to 1970-2001 based on inverse modeling.

570 For the interannual trends observed at Jungfraujoch, it is noteworthy to point out that our
571 observations covering a rather short period may lead to large uncertainties despite statistical
572 significance. The discrepancy found in the trends between the first and second phases indicates
573 that variability of N_2O isotopic composition is likely to obscure interannual trends over shorter
574 periods (Toyoda et al., 2013). Hence, extended time-series of isotopic measurements are needed
575 to reevaluate, for example, the observed tendency of increase in $\delta^{18}O$ and $\delta^{15}N^{SP}$ at Jungfraujoch
576 (Table 1; only significant during the first phase). For $\delta^{18}O$ of atmospheric N_2O, a generally
577 declining trend smaller than that of $\delta^{15}N^{bulk}$ has been indicated by a number of observations
578 (Bernard et al., 2006; Ishijima et al., 2007; Park et al., 2012; Röckmann et al., 2003; Röckmann
579 and Levin, 2005). This is expected as $\delta^{18}O$ of anthropogenic N_2O is not much different from that
580 of the natural background, ~~given~~ assuming that the oxygen atom in N_2O is largely derived from
581 soil water and ambient oxygen during production (Rahn and Wahlen, 2000).

582 It is still a challenging task to disentangle interannual trends of $\delta^{15}N^{SP}$-N_2O in the background
583 atmosphere, due to limitations in analytical repeatability and precision (Harris et al., 2017; Mohn
584 et al., 2014). Past results have reached inconsistent conclusions, showing positive (Bernard et al.,
585 2006; Park et al., 2012; Prokopiou et al., 2017; Röckmann and Levin, 2005) or negative
586 (Röckmann et al., 2003; Toyoda et al., 2013) trends of similar magnitude (Fig. ~~6~~7). On the one
587 hand, the negative trend in $\delta^{15}N^{SP}$ could be explained by the significantly lower $\delta^{15}N^{SP}$ from

anthropogenic sources (e.g. agricultural sources; Table ~~S2~~S1) than of the tropospheric background (near 18‰; Fig. ~~6~~7). On the other hand, Park et al. (2012) suggested that the increase of $\delta^{15}N^{SP}$ in the atmospheric N_2O may reflect a global increase in importance of the contribution by nitrification (high- $\delta^{15}N^{SP}$ process) to agricultural N_2O emissions. This is based on the assumption that the growth of N_2O emissions is largely due to enhanced fertilizer application which promotes nitrification activity (Pérez et al., 2001; Tian et al., 2018). The observed mean increase rate of 0.02‰ a^{-1} for $\delta^{15}N^{SP}$ by Park et al. (2012) could then be translated into an increase of 13-23% for the relative amount of nitrification-derived N_2O between 1750 and 2005. However, this should be further evaluated with more frequent sampling (Park et al. (2012) only sampled 1-6 times per year) and tested with isotopic measurements across the NH, where agricultural N_2O emissions are more dominant than in the SH. In addition, the strong seasonal pattern of $\delta^{15}N^{SP}$ at Jungfraujoch suggests that seasonal variations of $\delta^{15}N^{SP}$ in response to climatic or source factors are crucial and must be taken into consideration for evaluating interannual $\delta^{15}N^{SP}$ trends.

4.4 Simulated anthropogenic N_2O sources with the two-box model and comparison with other studies

To further evaluate anthropogenic source signatures of N_2O isotopic composition, we applied a two-box model representing a well-mixed troposphere and stratosphere (Röckmann et al., 2003; Schilt et al., 2014; Sowers et al., 2002). The model runs with the whole dataset (Table 2) and the dataset filtered for free-troposphere only ~~dataset~~ (Table S3) exhibit statistically identical results, supporting that our model estimates, with observations at Jungfraujoch, ~~is~~are representative of the background atmosphere. The simulated trends of the N_2O mixing ratios and isotopic composition show a gradual increase in N_2O and decrease in the isotopic signatures (see Fig. ~~6~~7), which agree with existing observations within the model uncertainty. However, this does not hold for individual

studies considered separately. For example, the N_2O mixing ratios observed by Röckmann et al. (2003) and Prokopiou et al. (2017) would lead to a higher preindustrial N_2O compared to our model simulation, which is likely due to the uncertainty in the firn air records (Prokopiou et al., 2017).

We compared the anthropogenic isotopic signatures determined by our two-box model with other similar studies in Table 2. Our estimates generally lie within the ranges given in the earlier studies (Ishijima et al., 2007; Park et al., 2012; Prokopiou et al., 2017; Sowers et al., 2002; Toyoda et al., 2013). However, isotopic signatures of N_2O sources estimated for 2018 in this study are higher in $\delta^{15}N^{bulk}$ and $\delta^{18}O$ (by 4-8‰), and lower in $\delta^{15}N^{SP}$ (by 2-7‰) than model estimates for the early 2000s from two other studies from SH (Park et al., 2012; Prokopiou et al., 2017). Such differences in $\delta^{15}N^{bulk}$ and $\delta^{18}O$ could be related to interhemispheric differences, as the relative contributions of N_2O sources vary between the two hemispheres (Toyoda et al., 2013). Also, more interestingly, this could suggest a shift in the N_2O source isotopic signatures over the last few decades. For example, an increase of $\delta^{15}N^{bulk}$ in anthropogenic N_2O sources over time may be attributed to growing contributions of other industrial/waste sources with high $\delta^{15}N^{bulk}$ (Prokopiou et al., 2017). In addition, if the assumption of increasing $\delta^{15}N^{bulk}$ and decreasing $\delta^{15}N^{SP}$ in anthropogenic N_2O sources over time holds, it points to a recently growing contribution of denitrification relative to nitrification, to the global atmospheric N_2O increase (Sutka et al., 2006; Toyoda et al., 2013). ~~This does not necessarily contradict~~By contrast, Park et al. (2012) ~~or~~ and Prokopiou et al. (2017) ~~, who~~ proposed an increasing importance of nitrification for anthropogenic N_2O emissions based on the increasing $\delta^{15}N^{SP}$ trend since 1940~~,~~. This may suggest~~as~~ that ~~the change in N_2O source processes in recent decades may instead reflect~~ a strong~~er~~ climate change feedback has recently resulted in significant shifts in N_2O source process, hence twisting the isotopic signatures of anthropogenic

sources (Griffis et al., 2017; Xu-Ri et al., 2012). Alternatively, the uncertainty in determining N_2O isotopic signatures in the background atmosphere and inter-laboratory comparability may play a role in the observed discrepancy.

Given the strong heterogeneity in source contributions to N_2O emissions around the globe (Saikawa et al., 2014), current two- and four-box model estimates based on observations at individual sites or regions are likely to reflect latitudinal or even interhemispheric differences in anthropogenic isotopic signatures. On the other hand, previous discussions of the model sensitivities by Röckmann et al. (2003) and Toyoda et al. (2013) have suggested that anthropogenic isotopic values are most sensitive to the trends in tropospheric isotopic values ~~as well as~~and the relative difference in tropospheric isotopic values between present and preindustrial times. ~~As shown in Figure 6~~For example, given the similar parameters used for preindustrial times as our study, Park et al. (2012) observed much lower $\delta^{15}N^{bulk}$ in the recent troposphere than in our case, hence resulting in significantly lower $\delta^{15}N^{bulk}$ for the anthropogenic source. Furthermore, ~~and both~~ Park et al. (2012) and Prokopiou et al. (2017) ~~found~~ simulated a positive trend in $\delta^{15}N^{SP}$~~.~~ relative to preindustrial times, which in return ~~computed~~resulted in a much higher $\delta^{15}N^{SP}$ for the anthropogenic sources. ~~These may help to explain some differences in anthropogenic source signatures between our and their box model estimates.~~

Using an alternative bottom-up approach, we estimated the anthropogenic source isotopic signatures based on the N_2O emission inventory simulated for Jungfraujoch and published source isotopic signatures as summarized by Harris et al. (2017) (Table ~~S2~~S1). The retrieved anthropogenic isotopic signatures (Table 3) were largely in agreement with the isotopic signature of agricultural soil emissions (Snider et al., 2015b; Wolf et al., 2015), indicating that this source could explain more than 60% of the total N_2O emissions. However, the anthropogenic isotopic

657 signatures estimated by this approach were lower than the results from our two-box model (Table
658 2). In contrast, another similar bottom-up estimate based on the global N_2O emission inventory
659 (Toyoda et al., 2013) reported anthropogenic isotopic values that agree well with our box-model
660 results. This may be explained by the different isotopic signatures used to describe agricultural
661 N_2O emissions, as those values used for the bottom-up estimates by Toyoda et al. (2013) were
662 significantly lower (Toyoda et al., 2011) than those used in this study (Snider et al., 2015b; Wolf
663 et al., 2015). Such bottom-up estimation suggests that more isotopic measurements of the
664 background atmosphere from different regions, and better constraints on individual anthropogenic
665 (especially agricultural) N_2O isotopic signatures, are necessary for a better representation of N_2O
666 isotopic composition in atmospheric modeling studies.

5 Conclusions

With the recently developed laser spectroscopic technique coupled with a preconcentration device, we achieved good repeatability in measurements of N_2O isotopic composition from the background atmosphere at Jungfraujoch, Switzerland. This time-series covered a period of five years and showed a distinct seasonality, with $\delta^{15}N^{bulk}$ maxima and $\delta^{15}N^{SP}$ minima in late summer, associated with the lowest N_2O mixing ratios over the year. The seasonal fluctuation of $\delta^{15}N^{bulk}$ was associated with the stratosphere-troposphere exchange process, in agreement with other monitoring networks (Nevison et al., 2011), while the contrasting depletion of $\delta^{15}N^{SP}$ in later summer is possibly a combined result of STE and agricultural emissions, with the latter being more important. The analyses of air mass transport regimes together with the simulation of N_2O enhancements for Jungfraujoch supported our explanations and highlighted that the fluctuation between the free troposphere and local contributions dominated by soil emission drives the seasonality of $\delta^{15}N^{SP}$ and $\delta^{18}O$ as observed at Jungfraujoch.

We found statistically significant interannual trends for $\delta^{15}N^{bulk}$, which is expected as anthropogenic N_2O sources are characterized by low ^{15}N abundance. For $\delta^{15}N^{SP}$ and $\delta^{18}O$, interannual trends were highly uncertain and possibly masked by ~~higher-frequency~~their large temporal variabilities~~tion~~. Using a two-box model approach, we simulated the evolution of N_2O isotopic composition from preindustrial times to the present. This model suggests an overall decreasing trend for all isotopic species in conjunction with the atmospheric N_2O increase. The anthropogenic source signatures given by the model generally agreed with previous studies. However, these model results are still sensitive to the ranges and trends of the observed N_2O isotopic signatures in the present troposphere. In the future, more extended records of high-precision N_2O isotopic measurements and application of multiple-box modeling approaches

690 (Rigby et al., 2013) are necessary to account for the global N_2O budget and evolution of
691 anthropogenic sources.

Data availability

Data for N_2O mixing ratios and isotopic composition of flask samples at Jungfraujoch could be found in the supplementary materials. *In situ* data for N_2O mixing ratios at Jungfraujoch are available from World Data Centre for Greenhouse Gases (WMO-GAW; https://gaw.kishou.go.jp). Other data are available upon request through the corresponding author (longfei.yu@empa.ch).

Author contribution:

LY, EH and JM led and designed this study. LY, EH, SE conducted sample collection at Jungfraujoch; LY and EH analyzed discrete samples at Empa; MS and CZ contributed *in situ* measurements of N_2O, NO_y, CO and O_3 at Jungfraujoch; LY, EH and SH performed data analyses for the time-series and conducted model simulations. LY wrote the main manuscript; EH, SH and JM were involved in the revisions of the manuscript and commenting. SE, MS, LE and CZ were also involved in scientific discussion and commenting on the manuscript.

Competing interests

The authors declare that they have no conflict of interest.

Acknowledgements

We are thankful to the research infrastructure provided by the High Altitude Research Stations Jungfraujoch and Gornergrat. We are grateful to the help from the custodians (Mr. and Mrs. Fischer and Mr. and Mrs. Käser) at the research station of Jungfraujoch. We would like to thank Simon Wyss, Kerstin Zeyer, Patrik Zanchetta and Flurin Dietz for their support with the sample collection as well as laboratory assistance. The NABEL network is operated by Empa in collaboration with the Swiss Federal Office for the Environment. Prof. Sakae Toyoda and Prof. Naohiro Yoshida from Tokyo Institute of Technology are acknowledged for their analyses of the applied reference

714 standards. This study was financially supported by the Swiss National Science Foundation (grant
715 number 200021_163075) and the Swiss contribution to the Integrated Carbon Observation System
716 (ICOS) Research Infrastructure (ICOS-CH). ICOS-CH is funded by the Swiss National Science
717 Foundation and in-house contributions. Longfei Yu was additionally supported by the
718 EMPAPOSTDOCS-II program, which receives funding from the European Union's Horizon 2020
719 research and innovation program under the Marie Skłodowska-Curie grant agreement number
720 754364.

721

References

Appenzeller, C., Begert, M., Zenklusen, E. and Scherrer, S. C.: Monitoring climate at Jungfraujoch in the high Swiss Alpine region, Sci. Total Environ., 391(2–3), 262–268, doi:10.1016/j.scitotenv.2007.10.005, 2008.

Bernard, S., Röckmann, T., Kaiser, J., Barnola, J.-M., Fischer, H., Blunier, T. and Chappellaz, J.: Constraints on N_2O budget changes since pre-industrial time from new firn air and ice core isotope measurements, Atmos. Chem. Phys. Discuss., 5(4), 7547–7575, doi:10.5194/acpd-5-7547-2005, 2006.

Bourbonnais, A., Letscher, R. T., Bange, H. W., Échevin, V., Larkum, J., Mohn, J., Yoshida, N. and Altabet, M. A.: N_2O production and consumption from stable isotopic and concentration data in the Peruvian coastal upwelling system, Global Biogeochem. Cycles, 31(4), 678–698, doi:10.1002/2016GB005567, 2017.

Buchmann, B., Hueglin, C., Reimann, S., Vollmer, M. K., Steinbacher, M. and Emmenegger, L.: Reactive gases, ozone depleting substances and greenhouse gases, in From weather observations to atmospheric and climate sciences in Switzerland, edited by S. Willemse and M. Furger, vdf Hochschulverlag AG., 2016.

Bukowiecki, N., Weingartner, E., Gysel, M., Coen, M. C., Zieger, P., Herrmann, E., Steinbacher, M., Gäggeler, H. W. and Baltensperger, U.: A review of more than 20 years of aerosol observation at the high altitude research station Jungfraujoch, Switzerland (3580 m asl), Aerosol Air Qual. Res., 16(3), 764–788, doi:10.4209/aaqr.2015.05.0305, 2016.

Butterbach-Bahl, K., Baggs, E. M., Dannenmann, M., Kiese, R. and Zechmeister-Boltenstern, S.: Nitrous oxide emissions from soils: how well do we understand the processes and their controls?, Philos. Trans. R. Soc. Lond. B. Biol. Sci., 368, 20130122, doi:10.1098/rstb.2013.0122, 2013.

Decock, C. and Six, J.: How reliable is the intramolecular distribution of ^{15}N in N_2O to source partition N_2O emitted from soil?, Soil Biol. Biochem., 65(2), 114–127, doi:10.1016/j.soilbio.2013.05.012, 2013.

Denk, T. R. A., Mohn, J., Decock, C., Lewicka-Szczebak, D., Harris, E., Butterbach-Bahl, K., Kiese, R. and Wolf, B.: The nitrogen cycle: A review of isotope effects and isotope modeling approaches, Soil Biol. Biochem., 105, 121–137, doi:10.1016/j.soilbio.2016.11.015, 2017.

Denk, T. R. A., Kraus, D., Kiese, R., Butterbach-Bahl, K. and Wolf, B.: Constraining N cycling in the ecosystem model LandscapeDNDC with the stable isotope model SIMONE, Ecology, 100(5), c02675, doi:10.1002/ecy.2675, 2019.

Fowler, D., Steadman, C. E., Stevenson, D., Coyle, M., Rees, R. M., Skiba, U. M., Sutton, M. a., Cape, J. N., Dore, a. J., Vieno, M., Simpson, D., Zaehle, S., Stocker, B. D., Rinaldi, M., Facchini, M. C., Flechard, C. R., Nemitz, E., Twigg, M., Erisman, J. W. and Galloway, J. N.: Effects of global change during the 21st century on the nitrogen cycle, Atmos. Chem. Phys. Discuss., 15(2), 1747–1868, doi:10.5194/acpd-15-1747-2015, 2015.

Fujii, A., Toyoda, S., Yoshida, O., Watanabe, S., Sasaki, K. and Yoshida, N.: Distribution of nitrous oxide dissolved in water masses in the eastern subtropical North Pacific and its origin inferred from isotopomer analysis, J. Oceanogr., 69(2), 147–157, doi:10.1007/s10872-012-0162-4, 2013.

Griffis, T. J., Chen, Z., Baker, J. M., Wood, J. D., Millet, D. B., Lee, X., Venterea, R. T. and Turner, P. A.: Nitrous oxide emissions are enhanced in a warmer and wetter world, Proc. Natl. Acad. Sci., 201704552, doi:10.1073/pnas.1704552114, 2017.

Hall, B. D., Dutton, G. S. and Elkins, J. W.: The NOAA nitrous oxide standard scale for atmospheric observations, J. Geophys. Res. Atmos., 112(9), 1–9, doi:10.1029/2006JD007954, 2007.

765 Harris, E., Ibraim, E., Henne, S., Hüglin, C., Zellweger, C., Tuzson, B., Emmenegger, L. and Mohn, J.:
766 Tracking nitrous oxide emission processes at a suburban site with semicontinuous , in situ measurements
767 of isotopic composition, J. Geophys. Res. Atmos., 122, 1850–1870, doi:10.1002/2016JD025906, 2017.

768 Harris, E. J., Nelson, D. D., Olsewski, W., Zahniser, M., Potter, E., Mcmanus, B. J., Whitehill, A., Prinn,
769 R. G., Ono, S. and Harris, E.: Development of a spectroscopic technique for continuous online monitoring
770 of oxygen and site-specific nitrogen isotopic com, Anal. Chem., 86(3), 1726–1734, 2014.

771 Heil, J., Wolf, B., Brüggemann, N., Emmenegger, L., Tuzson, B., Vereecken, H. and Mohn, J.: Site-
772 specific 15N isotopic signatures of abiotically produced N_2O, Geochim. Cosmochim. Acta, 139, 72–82,
773 doi:10.1016/j.gca.2014.04.037, 2014.

774 Henne, S., Brunner, D., Folini, D., Solberg, S., Klausen, J. and Buchmann, B.: Assessment of parameters
775 describing representativeness of air quality in-situ measurement sites, Atmos. Chem. Phys., 10(8), 3561–
776 3581, doi:10.5194/acp-10-3561-2010, 2010.

777 Henne, S., Brunner, D., Oney, B., Leuenberger, M., Eugster, W., Bamberger, I., Meinhardt, F.,
778 Steinbacher, M. and Emmenegger, L.: Validation of the Swiss methane emission inventory by
779 atmospheric observations and inverse modelling, Atmos. Chem. Phys., 16(6), 3683–3710,
780 doi:10.5194/acp-16-3683-2016, 2016.

781 Henne, S., Mohn, J. and Brunner, D.: Quantification of Swiss nitrous oxide emissions through
782 atmospheric observations and inverse modelling, Final Report, Project of FOEN, 2019.

783 Herrmann, E., Weingartner, E., Henne, S., Vuilleumier, L., Bukowiecki, N., Steinbacher, M., Conen, F.,
784 Coen, M. C., Hammer, E., Juranyi, Z., Baltensperger, U. and Gysel, M.: Analysis of long-term aerosol
785 size distribution data from Jungfraujoch with emphasis on free tropospheric conditions, cloud influence,
786 and air mass transport, J. Geophys. Res. Atmos., 120, 1751–1762, doi:10.1002/2015JD023660, 2015.

787 Ibraim, E., Wolf, B., Harris, E., Gasche, R., Wei, J., Yu, L., Kiese, R., Eggleston, S., Butterbach-Bahl, K.,
788 Zeeman, M., Tuzson, B., Emmenegger, L., Six, J., Henne, S. and Mohn, J.: Attribution of N_2O sources in
789 a grassland soil with laser spectroscopy based isotopocule analysis, Biogeosciences, 16, 3247–3266,
790 doi.org/10.5194/bg-16-3247-2019, 2019.

791 Ishijima, K., Sugawara, S., Kawamura, K., Hashida, G., Morimoto, S., Murayama, S., Aoki, S. and
792 Nakazawa, T.: Temporal variations of the atmospheric nitrous oxide concentration and its $\delta^{15}N$ and $\delta^{18}O$
793 for the latter half of the 20th century reconstructed from firn air analyses, J. Geophys. Res. Atmos.,
794 112(3), doi:10.1029/2006JD007208, 2007.

795 Janssens-Maenhout, G., Crippa, M., Guizzardi, D., Muntean, M., Schaaf, E., Dentener, F., Bergamaschi,
796 P., Pagliari, V., Olivier, J., Peters, J., van Aardenne, J., Monni, S., Doering, U., Petrescu, R., Solazzo, E.
797 and Oreggioni, G.: EDGAR v4.3.2 Global Atlas of the three major Greenhouse Gas Emissions for the
798 period 1970-2012, Earth Syst. Sci. Data Discuss., 2010, 1–52, doi:10.5194/essd-2018-164, 2019.

799 Jiang, X., Ku, W. L., Shia, R. L., Li, Q., Elkins, J. W., Prinn, R. G. and Yung, Y. L.: Seasonal cycle of
800 N_2O: Analysis of data, Global Biogeochem. Cycles, 21, GB1006, doi:10.1029/2006GB002691, 2007.

801 JMA and WMO: World Meteorological Organization - Global Atmosphere Watch - World Data Centre
802 for Greenhouse Gases, Data Summary, No. 42, 101 p.,. [online] Available from:
803 https://gaw.kishou.go.jp/static/publications/summary/sum42/sum42.pdf, 2018.

804 Kaiser, J., Röckmann, T. and Brenninkmeijer, C. A. M.: Complete and accurate mass spectrometric
805 isotope analysis of tropospheric nitrous oxide, J. Geophys. Res. Atmos., 108, 4476,
806 doi:10.1029/2003JD003613, D15.

807 Keller, C. A., Hill, M., Vollmer, M. K., Henne, S., Brunner, D., Reimann, S., O'Doherty, S., Arduini, J.,
808 Maione, M., Ferenczi, Z., Haszpra, L., Manning, A. J. and Peter, T.: European emissions of halogenated
809 greenhouse gases inferred from atmospheric measurements, Environ. Sci. Technol., 46(1), 217–225,

doi:10.1021/es202453j, 2012.

Kim, K.-R. and Craig, H.: Nitrogen-15 and Oxygen-18 Characacteristics of Nitrous Oxide: A Global Perspective, Science , 262, 1855-1857, 1993.

Lebegue, B., Schmidt, M., Ramonet, M., Wastine, B., Yver Kwok, C., Laurent, O., Belviso, S., Guemri, A., Philippon, C., Smith, J. and Conil, S.: Comparison of nitrous oxide (N_2O) analyzers for high-precision measurements of atmospheric mole fractions, Atmos. Meas. Tech., 9(3), 1221–1238, doi:10.5194/amt-9-1221-2016, 2016.

Logan, J. A., Staehelin, J., Megretskaia, I. A., Cammas, J. P., Thouret, V., Claude, H., De Backer, H., Steinbacher, M., Scheel, H. E., Stbi, R., Frhlich, M. and Derwent, R.: Changes in ozone over Europe: Analysis of ozone measurements from sondes, regular aircraft (MOZAIC) and alpine surface sites, J. Geophys. Res. Atmos., 117(9), 1–23, doi:10.1029/2011JD016952, 2012.

Mohn, J., Guggenheim, C., Tuzson, B., Vollmer, M. K., Toyoda, S., Yoshida, N. and Emmenegger, L.: A liquid nitrogen-free preconcentration unit for measurements of ambient N_2O isotopomers by QCLAS, Atmos. Meas. Tech., 3(3), 609–618, doi:10.5194/amt-3-609-2010, 2010.

Mohn, J., Tuzson, B., Manninen, A., Yoshida, N., Toyoda, S., Brand, W. A. and Emmenegger, L.: Site selective real-time measurements of atmospheric N2O isotopomers by laser spectroscopy, Atmos. Meas. Tech., 5(7), 1601–1609, doi:10.5194/amt-5-1601-2012, 2012.

Mohn, J., Wolf, B., Toyoda, S., Lin, C. T., Liang, M. C., Brüggemann, N., Wissel, H., Steiker, A. E., Dyckmans, J., Szwec, L., Ostrom, N. E., Casciotti, K. L., Forbes, M., Giesemann, A., Well, R., Doucett, R. R., Yarnes, C. T., Ridley, A. R., Kaiser, J. and Yoshida, N.: Interlaboratory assessment of nitrous oxide isotopomer analysis by isotope ratio mass spectrometry and laser spectroscopy: Current status and perspectives, Rapid Commun. Mass Spectrom., 28(18), 1995–2007, doi:10.1002/rcm.6982, 2014.

Nevison, C. D., Keeling, R. F., Weiss, R. F., Popp, B. N., Jin, X., Fraser, P. J., Porter, L. W. and Hess, P. G.: Southern Ocean ventilation inferred from seasonal cycles of atmospehric N_2O and O_2/N_2 at Cape Grim, Tasmania, Tellus, Ser. B Chem. Phys. Meteorol., 57(3), 218–229, doi:10.1111/j.1600-0889.2005.00143.x, 2005.

Nevison, C. D., Dlugokencky, E., Dutton, G., Elkins, J. W., Fraser, P., Hall, B., Krummel, P. B., Langenfelds, R. L., O'Doherty, S., Prinn, R. G., Steele, L. P. and Weiss, R. F.: Exploring causes of interannual variability in the seasonal cycles of tropospheric nitrous oxide, Atmos. Chem. Phys., 11(8), 3713–3730, doi:10.5194/acp-11-3713-2011, 2011.

Ogawa, M. and Yoshida, N.: Intramolecular distribution of stable nitrogen and oxygen isotopes of nitrous oxide emitted during coal combustion, Chemosphere, 61(6), 877–887, doi:10.1016/j.chemosphere.2005.04.096, 2005.

Ostrom, N. E., Gandhi, H., Coplen, T. B., Toyoda, S., Böhlke, J. K., Brand, W. A., Casciotti, K. L., Dyckmans, J., Giesemann, A., Mohn, J., Well, R., Yu, L. and Yoshida, N.: Preliminary assessment of stable nitrogen and oxygen isotopic composition of USGS51 and USGS52 nitrous oxide reference gases and perspectives on calibration needs, Rapid Commun. Mass Spectrom., 32(15), 1207–1214, doi:10.1002/rcm.8157, 2018.

Pandey Deolal, S., Brunner, D., Steinbacher, M., Weers, U. and Staehelin, J.: Long-term in situ measurements of NO_x and NO_y at Jungfraujoch 1998-2009: Time series analysis and evaluation, Atmos. Chem. Phys., 12(5), 2551–2566, doi:10.5194/acp-12-2551-2012, 2012.

Park, S., Croteau, P., Boering, K. A., Etheridge, D. M., Ferretti, D., Fraser, P. J., Kim, K.-R., Krummel, P. B., Langenfelds, R. L., van Ommen, T. D., Steele, L. P. and Trudinger, C. M.: Trends and seasonal cycles in the isotopic composition of nitrous oxide since 1940, Nat. Geosci., 5(4), 261–265, doi:10.1038/ngeo1421, 2012.

Pérez, T., Trumbore, S. E., Tyler, S. C., Matson, P. A., I., O.-M., Rahn, T. and Griffiths, D. W. T.: Identifying the agricultural imprint on the global N2O budget using stable isotopes, J. Geophys. Res., 106, 9869–9878, doi:10.1179/1607845413y.0000000087, 2001.

Prather, M. J., Hsu, J., Deluca, N. M., Jackman, C. H., Oman, L. D., Douglass, A. R., Fleming, E. L., Strahan, S. E., Steenrod, S. D., Søvde, O. A., Isaksen, I. S. A., Froidevaux, L. and Funke, B.: Measuring and modeling the lifetime of nitrous oxide including its variability Michael, J. Geophys. Res. Atmos., 120, 5693–5705, doi:10.1002/2015JD023267.Received, 2015.

Prinn, R. G., Weiss, R. F., Arduini, J., Arnold, T., Dewitt, H. L., Fraser, P. J., Ganesan, A. L., Gasore, J., Harth, C. M., Hermansen, O., Kim, J., Krummel, P. B., Li, S., Loh, Z. M., Lunder, C. R. and Maione, M.: History of chemically and radiatively important atmospheric gases from the Advanced Global Atmospheric Gases Experiment (AGAGE), Earth Syst. Sci. Data, 10, 985–1018, 2018.

Prokopiou, M., Martinerie, P., Sapart, C. J., Witrant, E., Monteil, G. A., Ishijima, K., Bernard, S., Kaiser, J., Levin, I., Sowers, T., Blunier, T., Etheridge, D., Dlugokencky, E., van de Wal, R. S. W. and Röckmann, T.: Constraining N_2O emissions since 1940 using firn air isotope measurements in both hemispheres, Atmos. Chem. Phys., 2011(June), 1–50, doi:10.5194/acp-2016-487, 2017.

Prokopiou, M., Sapart, C. J., Rosen, J., Sperlich, P., Blunier, T., Brook, E., van de Wal, R. S. W. and Röckmann, T.: Changes in the Isotopic Signature of Atmospheric Nitrous Oxide and Its Global Average Source During the Last Three Millennia, J. Geophys. Res. Atmos., 1–17, doi:10.1029/2018JD029008, 2018.

Rahn, T. and Wahlen, M.: A reassessment of the global isotopic budget of atmospheric nitrous oxide, Global Biogeochem. Cycles, 14(2), 537–543, doi:10.1029/1999GB900070, 2000.

Ravishankara, A. R., Daniel, J. S. and Portmann, R. W.: Nitrous oxide (N_2O): the dominant ozone-depleting substance emitted in the 21st century., Science, 326(5949), 123–5, doi:10.1126/science.1176985, 2009.

Reay, D. S., Davidson, E. a., Smith, K. a., Smith, P., Melillo, J. M., Dentener, F. and Crutzen, P. J.: Global agriculture and nitrous oxide emissions, Nat. Clim. Chang., 2(6), 410–416, doi:10.1038/nclimate1458, 2012.

Reimann, S., Vollmer, M. K., Folini, D., Steinbacher, M., Hill, M., Buchmann, B., Zander, R. and Mahieu, E.: Observations of long-lived anthropogenic halocarbons at the high-Alpine site of Jungfraujoch (Switzerland) for assessment of trends and European sources, Sci. Total Environ., 391(2–3), 224–231, doi:10.1016/j.scitotenv.2007.10.022, 2008.

Rigby, M., Prinn, R. G., O'Doherty, S., Montzka, S. A., McCulloch, A., Harth, C. M., Mühle, J., Salameh, P. K., Weiss, R. F., Young, D., Simmonds, P. G., Hall, B. D., Dutton, G. S., Nance, D., Mondeel, D. J., Elkins, J. W., Krummel, P. B., Steele, L. P. and Fraser, P. J.: Re-evaluation of the lifetimes of the major CFCs and CH3CCl3 using atmospheric trends, Atmos. Chem. Phys., 13(5), 2691–2702, doi:10.5194/acp-13-2691-2013, 2013.

Röckmann, T., Kaiser, J. and Brenninkmeijer, C. A. M.: The isotopic fingerprint of the pre-industrial and the anthropogenic N_2O source, Atmos. Chem. Phys., (3), 315–323, 2003.

Röckmann, T. and Levin, I.: High-precision determination of the changing isotopic composition of atmospheric N_2O from 1990 to 2002, J. Geophys. Res. Atmos., 110(21), 1–8, doi:10.1029/2005JD006066, 2005.

Saikawa, E., Prinn, R. G., Dlugokencky, E., Ishijima, K., Dutton, G. S., Hall, B. D., Langenfelds, R., Tohjima, Y., Machida, T., Manizza, M., Rigby, M., O'Doherty, S., Patra, P. K., Harth, C. M., Weiss, R. F., Krummel, P. B., Van Der Schoot, M., Fraser, P. J., Steele, L. P., Aoki, S., Nakazawa, T. and Elkins, J. W.: Global and regional emissions estimates for N_2O, Atmos. Chem. Phys., 14(9), 4617–4641,

900 doi:10.5194/acp-14-4617-2014, 2014.

901 Schibig, M. F., Steinbacher, M., Buchmann, B., Van Der Laan-Luijkx, I. T., Van Der Laan, S., Ranjan, S.
902 and Leuenberger, M. C.: Comparison of continuous in situ CO_2 observations at Jungfraujoch using two
903 different measurement techniques, Atmos. Meas. Tech., 8(1), 57–68, doi:10.5194/amt-8-57-2015, 2015.

904 Schilt, A., Brook, E. J., Bauska, T. K., Baggenstos, D., Fischer, H., Joos, F., Petrenko, V. V., Schaefer,
905 H., Schmitt, J., Severinghaus, J. P., Spahni, R. and Stocker, T. F.: Isotopic constraints on marine and
906 terrestrial N_2O emissions during the last deglaciation, Nature, 516(7530), 234–237,
907 doi:10.1038/nature13971, 2014.

908 Sepúlveda, E., Schneider, M., Hase, F., Barthlott, S., Dubravica, D., García, O. E., Gomez-Pelaez, A.,
909 González, Y., Guerra, J.C., Gisi, M., Kohlhepp, R., Dohe, S., Blumenstock, T., Strong, K., Weaver, D.,
910 Palm, N., Sadeghi, A., Deutscher, N. M., Warneke, T., Notholt, J., Jones, N., Griffith, D. W. T., Smale,
911 D., Brailsford, G. W., Robinson, J., Meinhardt, F., Steinbacher, M., Aalto, T. and Worthy, D.:
912 Tropospheric CH_4 signals as observed by NDACC FTIR at globally distributed sites and comparison to
913 GAW surface in situ measurements, Atmos. Meas. Tech., 7(7), 2337–2360, doi:10.5194/amt-7-2337-
914 2014, 2014.

915 Snider, D., Thompson, K., Wagner-Riddle, C., Spoelstra, J. and Dunfield, K.: Molecular techniques and
916 stable isotope ratios at natural abundance give complementary inferences about N_2O production pathways
917 in an agricultural soil following a rainfall event, Soil Biol. Biochem., 88, 197–213,
918 doi:10.1016/j.soilbio.2015.05.021, 2015a.

919 Snider, D. M., Venkiteswaran, J. J., Schiff, S. L. and Spoelstra, J.: From the ground up: Global nitrous
920 oxide sources are constrained by stable isotope values, PLoS One, 10(3), 1–19,
921 doi:10.1371/journal.pone.0118954, 2015b.

922 Sowers, T., Rodebaugh, A., Yoshida, N. and Toyoda, S.: Extending records of the isotopic composition of
923 atmospheric N_2O back to 1800 A.D. from air trapped in snow at the South Pole and the Greenland Ice
924 Sheet Project II ice core, Global Biogeochem. Cycles, 16(4), 1–10, doi:10.1029/2002GB001911, 2002.

925 Stohl, A., Forster, C., Frank, A., Seibert, P. and Wotawa, G.: Technical note: The Lagrangian particle
926 dispersion model FLEXPART version 6.2, Atmos. Chem. Phys., 5, 2461–2474,
927 doi:10.3390/atmos9020076, 2005.

928 Sturm, P., Tuzson, B., Henne, S. and Emmenegger, L.: Tracking isotopic signatures of CO_2 at the high
929 altitude site Jungfraujoch with laser spectroscopy: Analytical improvements and representative results,
930 Atmos. Meas. Tech., 6(7), 1659–1671, doi:10.5194/amt-6-1659-2013, 2013.

931 Sutka, R. L., Ostrom, N. E., Ostrom, P. H., Breznak, J. a, Pitt, a J., Li, F. and Gandhi, H.: Distinguishing
932 Nitrous Oxide Production from Nitrification and Denitrification on the Basis of Isotopomer Abundances
933 Distinguishing Nitrous Oxide Production from Nitrification and Denitrification on the Basis of
934 Isotopomer Abundances, Appl. Environ. Microbiol., 72(1), 638–644, doi:10.1128/AEM.72.1.638, 2006.

935 Tarasova, O. A., Senik, I. A., Sosonkin, M. G., Cui, J., Staehelin, J. and Péevôt, A. S. H.: Surface ozone
936 at the Caucasian site Kislovodsk High Mountain Station and the Swiss Alpine site Jungfraujoch: Data
937 analysis and trends (1990-2006), Atmos. Chem. Phys., 9(12), 4157–4175, doi:10.5194/acp-9-4157-2009,
938 2009.

939 Team, R. C.: A language and environment for statistical computing. R Foundation for statistical
940 computing, 2015; Vienna, Austria, 2016.

941 Thompson, R. L., Patra, P. K., Ishijima, K., Saikawa, E., Corazza, M., Karstens, U., Wilson, C.,
942 Bergamaschi, P., Dlugokencky, E., Sweeney, C., Prinn, R. G., Weiss, R. F., O'Doherty, S., Fraser, P. J.,
943 Steele, L. P., Krummel, P. B., Saunois, M., Chipperfield, M. and Bousquet, P.: TransCom N_2O model
944 inter-comparison-Part 1: Assessing the influence of transport and surface fluxes on tropospheric N_2O

variability, Atmos. Chem. Phys., 14(8), 4349–4368, doi:10.5194/acp-14-4349-2014, 2014a.

Thompson, R. L., Ishijima, K., Saikawa, E., Corazza, M., Karstens, U., Patra, P. K., Bergamaschi, P., Chevallier, F., Dlugokencky, E., Prinn, R. G., Weiss, R. F., O'Doherty, S., Fraser, P. J., Steele, L. P., Krummel, P. B., Vermeulen, A., Tohjima, Y., Jordan, A., Haszpra, L., Steinbacher, M., Van Der Laan, S., Aalto, T., Meinhardt, F., Popa, M. E., Moncrieff, J. and Bousquet, P.: TransCom N_2O model inter-comparison - Part 2: Atmospheric inversion estimates of N_2O emissions, Atmos. Chem. Phys., 14(12), 6177–6194, doi:10.5194/acp-14-6177-2014, 2014b.

Thoning, K. W., Tans, P. P. and Komhyr, W. D.: Atmospheric carbon dioxide at Mauna Loa Observatory: 2. Analysis of the NOAA GMCC data, 1974-1985, J. Geophys. Res., 94(D6), 8549–8565, doi:10.1029/jd094id06p08549, 1989.

Tian, H., Yang, J., Xu, R., Lu, C., Canadell, J., Davidson, E. A., Jackson, R., Arneth, A., Chang, J., Ciais, P., Gerber, S., Ito, A., Joos, F., Lienert, S., Messina, P., Olin, S., Pan, S., Peng, C., Saikawa, E., Thompson, R., Vuichard, N., Winiwarter, W., Zaehle, S. and Zhang, B.: Global soil nitrous oxide emissions since the preindustrial era estimated by an ensemble of terrestrial biosphere models: Magnitude, attribution, and uncertainty, Glob. Chang. Biol., 25(2), 640–659, doi:10.1111/gcb.14514, 2018.

Toyoda, S., Yoshida, N., Urabe, T., Aoki, S., Nakazawa, T., Sugawara, S. and Honda, H.: Fractionation of N_2O isotopomers in the stratosphere, J. Geophys. Res., 106(D7), 7515, doi:10.1029/2000JD900680, 2001.

Toyoda, S., Yamamoto, S., Arai, S., Nara, H., Yoshida, N., Kashiwakura, K. and Akiyama, K.: Isotopomeric characterization of N2O produced, consumed, and emitted by automobiles, rapid comm, 22, 603–612, doi:10.1002/rcm, 2008.

Toyoda, S., Yano, M., Nishimura, S., Akiyama, H., Hayakawa, A., Koba, K., Sudo, S., Yagi, K., Makabe, A., Tobari, Y., Ogawa, N. O., Ohkouchi, N., Yamada, K. and Yoshida, N.: Characterization and production and consumption processes of N_2O emitted from temperate agricultural soils determined via isotopomer ratio analysis, Global Biogeochem. Cycles, 25(2), 1–17, doi:10.1029/2009GB003769, 2011.

Toyoda, S., Kuroki, N., Yoshida, N., Ishijima, K., Tohjima, Y. and Machida, T.: Decadal time series of tropospheric abundance of N_2O isotopomers and isotopologues in the Northern Hemisphere obtained by the long-term observation at Hateruma Island, Japan, J. Geophys. Res. Atmos., 118(8), 3369–3381, doi:10.1002/jgrd.50221, 2013.

Toyoda, S., Yoshida, N. and Koba, K.: Isotopocule analysis of biologically produced nitrous oxide in various environments, Mass Spectrom. Rev., (36), 135–160, doi:doi:10.1002/mas.21459, 2017.

Toyoda, S., Yoshida, N., Morimoto, S., Aoki, S., Nakazawa, T., Sugawara, S., Ishidoya, S., Uematsu, M., Inai, Y., Hasebe, F., Ikeda, C., Honda, H. and Ishijima, K.: Vertical distributions of N_2O isotopocules in the equatorial stratosphere, Atmos. Chem. Phys., (18), 833–844, 2018.

Tuzson, B., Henne, S., Brunner, D., Steinbacher, M., Mohn, J., Buchmann, B. and Emmenegger, L.: Continuous isotopic composition measurements of tropospheric CO_2 at Jungfraujoch (3580 m a.s.l.), Switzerland: Real-time observation of regional pollution events, Atmos. Chem. Phys., 11(4), 1685–1696, doi:10.5194/acp-11-1685-2011, 2011.

WMO: WMO Greenhouse Gas Bulletin., 2018.

Wolf, B., Merbold, L., Decock, C., Tuzson, B., Harris, E., Six, J., Emmenegger, L. and Mohn, J.: First on-line isotopic characterization of N2O above intensively managed grassland, Biogeosciences, 12(8), 2517–2531, doi:10.5194/bg-12-2517-2015, 2015.

Xu-Ri, Prentice, I. C., Spahni, R. and Niu, H. S.: Modelling terrestrial nitrous oxide emissions and implications for climate feedback, New Phytol., 196(2), 472–488, doi:10.1111/j.1469-8137.2012.04269.x,

2012.

Yoshida, N. and Toyoda, S.: Constraining the atmospheric N_2O budget from intramolecular site preference in N_2O isotopomers, Nature, 405(6784), 330–4, doi:10.1038/35012558, 2000.

Yuan, Y., Ries, L., Petermeier, H., Steinbacher, M., Gómez-Pelaéz, A. J., Leuenberger, M. C., Schumacher, M., Trickl, T., Couret, C., Meinhardt, F. and Menzel, A.: Adaptive selection of diurnal minimum variation: A statistical strategy to obtain representative atmospheric CO_2 data and its application to European elevated mountain stations, Atmos. Meas. Tech., 11(3), 1501–1514, doi:10.5194/amt-11-1501-2018, 2018.

Yung, Y. L. and Miller, C. E.: Isotopic fractionation of stratospheric nitrous oxide, Science, 278(5344), 1778–1780, doi:10.1126/science.278.5344.1778, 1997.

Zellweger, C., Forrer, J., Hofer, P., Nyeki, S., Schwarzenbach, B., Weingartner, E., Ammann, M. and Baltensperger, U.: Partitioning of reactive nitrogen (NO_y) and dependence on meteorological conditions in the lower free troposphere, Atmos. Chem. Phys., 3(3), 779–796, doi:10.5194/acp-3-779-2003, 2003.

Zellweger, C., Hüglin, C., Klausen, J., Steinbacher, M., Vollmer, M. and Buchmann, B.: Inter-comparison of four different carbon monoxide measurement techniques and evaluation of the long-term carbon monoxide time series of Jungfraujoch, Atmos. Chem. Phys., 9(11), 3491–3503, doi:10.5194/acp-9-3491-2009, 2009.

Table 1 Trends of amospheric $\delta^{15}N^{bulk}$, $\delta^{15}N^{SP}$ and $\delta^{18}O$ at Jungfraujoch determined using discrete measurements between April 2014 and December 2018. The trends are determined for the whole dataset, the dataset filtered for free troposphere (removing data points with significant influence from plenary boundary layer) and the second-phase dataset with bi-weekly measurements (August 2016 to December 2018).

	$\delta^{15}N^{bulk}$ (‰ a^{-1})		$\delta^{15}N^{SP}$ (‰ a^{-1})		$\delta^{18}O$ (‰ a^{-1})	
	Raw	Deseasonlized	Raw	Deseasonlized	Raw	Deseasonlized
Whole dataset	-0.059±0.012*	-0.052±0.012*	0.069±0.029	0.065±0.027	0.020±0.011	0.019±0.011
Free troposphere	-0.060±0.014*	-0.054±0.013*	0.054±0.034	0.036±0.030	0.024±0.013	0.019±0.011
First phase (Apr. 2014-Feb. 2016)	-0.036±0.038	-0.041±0.035	0.449±0.100*	0.314±0.082*	0.238±0.029*	0.207±0.026*
Second phase (Aug. 2016-Dec. 2018)	-0.105±0.049	-0.130±0.045*	0.028±0.067	-0.007±0.066	-0.007±0.042	-0.001±0.040

* Indicate significance of linear regression.

Table 2 Results of the two-box model simulations and selected literature values for comparison.

Variable	Anthropogenic source						
	This study	RMSE	Sowers et al. (2002)[a]	Ishijima et al. (2007)[b]	Toyoda et al. (2013)[c]	Park et al. (2012)[d]	Prokopiou et al. (2017)[e]
Air Sample Origin	NH[†]		FA, IC[†]	FA[†]	NH[†]	SH, FA[†]	FA[†]
	2014-2018		1745-1995	1960-2001	1999-2010	1940-2005	1940-2008
α *	0.0154±0.004	0.65 nmol mol^{-1}	0.0111 to 0.0128				
$F_{anth,2018}$ (TgN y^{-1})	8.6±0.6	NA	4.2 to 5.7		5.5	6.6	5.4±1.7
$\delta^{15}N^{bulk}$ (‰)	-8.6±4	0.23	-7 to -13	-11.6	-9.84	-15.6±1.2	-18.2±2.6
$\delta^{18}O$ (‰)	34.8±3	0.22	17 to 26		35.95	32.0±1.3	27.2±2.6
$\delta^{15}N^{SP}$ (‰)	10.7±4	0.50			8.52	13.1±9.4	18.0±8.6

[†] NH and SH: surface atmosphere from the Northern and Southern Hemisphere, respectively; FA: firn air; IC: ice core air.

* "Value" is the dimensionless constant α describing the exponential increase in the anthropogenic flux

φ RMSE refers to root mean square error. It is in nmol mol^{-1} for α, referring to the present day tropospheric mixing ratio for N_2O. For source isotopic values, RMSE is in the unit of ‰.

[a] Estimates are for 1995

[b] Estimate is for 2000, for $\delta^{18}O$ calibration is not comparable

[c] Estimates are for 2012 using the "Base" scenario

[d] Estimates are for 2005

[e] δ_{anth} values are averaged values for the period of 1940-2008.

Table 3 Isotopic signatures for the overall, anthropogenic and major N_2O sources contributing to N_2O variations at Jungfraujoch. Source signatures were estimated based on a "bottom-up" approach, with literature-derived isotopic signatures and fluxes for variable sources under the Swiss Meteotest emission inventory.

	Emission inventory (%)	$\delta^{15}N^{bulk}$ (‰)	$\delta^{15}N^{SP}$ (‰)	$\delta^{18}O$ (‰)	Reference
Overall source	100	-15.8 (6.2)	7.3 (3.9)	29.4 (5.5)	-
Anthropogenic source	89.4	-15.6 (6.3)	7.4 (4.0)	29.5 (5.7)	-
Agricultural emission	61.5	-17.8 (5.7)	7.2 (3.8)	29.0 (3.7)	Snider et al. (2015) Wolf et al. (2015)
Manure management	7.4	-17.5 (6.2)	6.5 (4.1)	23.9 (3.8)	Maeda et al. (2010)
Waste*	7.2	-11.5 (12.6)	10.4 (5.7)	31.3 (14.0)	Ogawa and Yoshida (2005) Snider et al. (2015)
Natural emission	10.9	-17.8 (5.7)	7.2 (3.8)	29.0 (3.7)	Snider et al. (2015) Wolf et al. (2015)

* "Waste" sources consist of both wastewater treatment and agricultural waste burning (biomass burning).

Figures

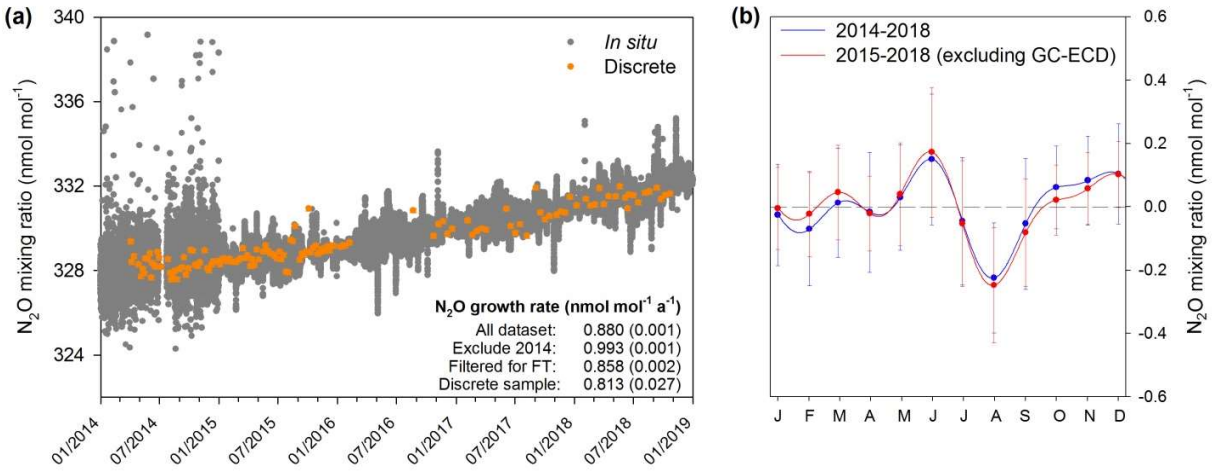

Figure 1a *In situ* (10-min averages) and discrete measurements of N_2O mixing ratios from April 2014 to December 2018 at Jungfraujoch. *In situ* N_2O mixing ratio measurements were performed with GC-ECD method between April and December 2014. After that, OA-ICOS became the major analytical method for *in situ* measurements. Discrete sample points are presented as averages with error bars (one standard deviation). Annual N_2O growth rates determined by linear regression are given in the figure (uncertainty shown as one standard deviation). A sampling gap exists for discrete samples between February and August 2016.

1b Seasonality of N_2O mixing ratios at Jungfraujoch derived from *in situ* measurements. Datasets with/without GC-ECD measurements are compared for seasonality evaluation. The NLS model simulation for time-series gives the detrended seasonality, with error bars indicating one standard deviation of monthly residuals.

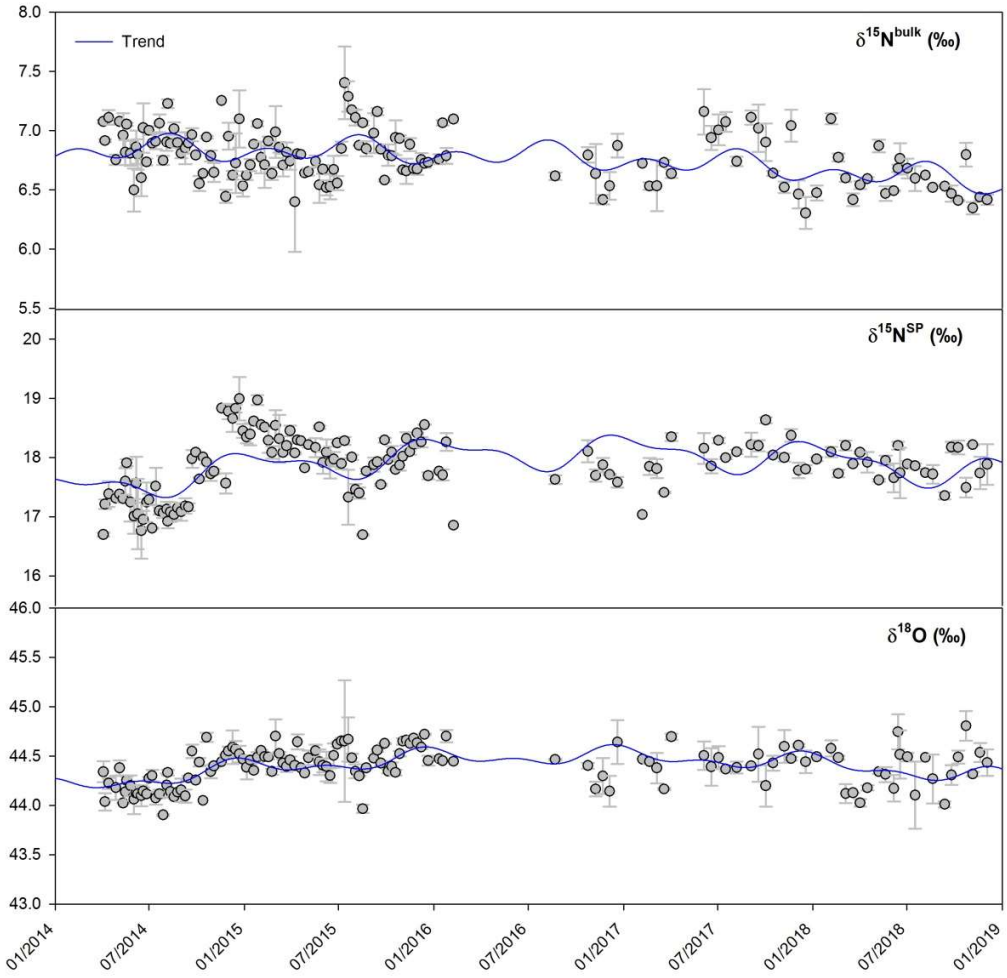

Figure 2 Time-series of isotopic composition of atmospheric N_2O observed at Jungfraujoch from April 2014 to December 2018. Error bars indicate one standard deviation of repeated measurements. Blue lines indicate the simulated trends by the NLS model.

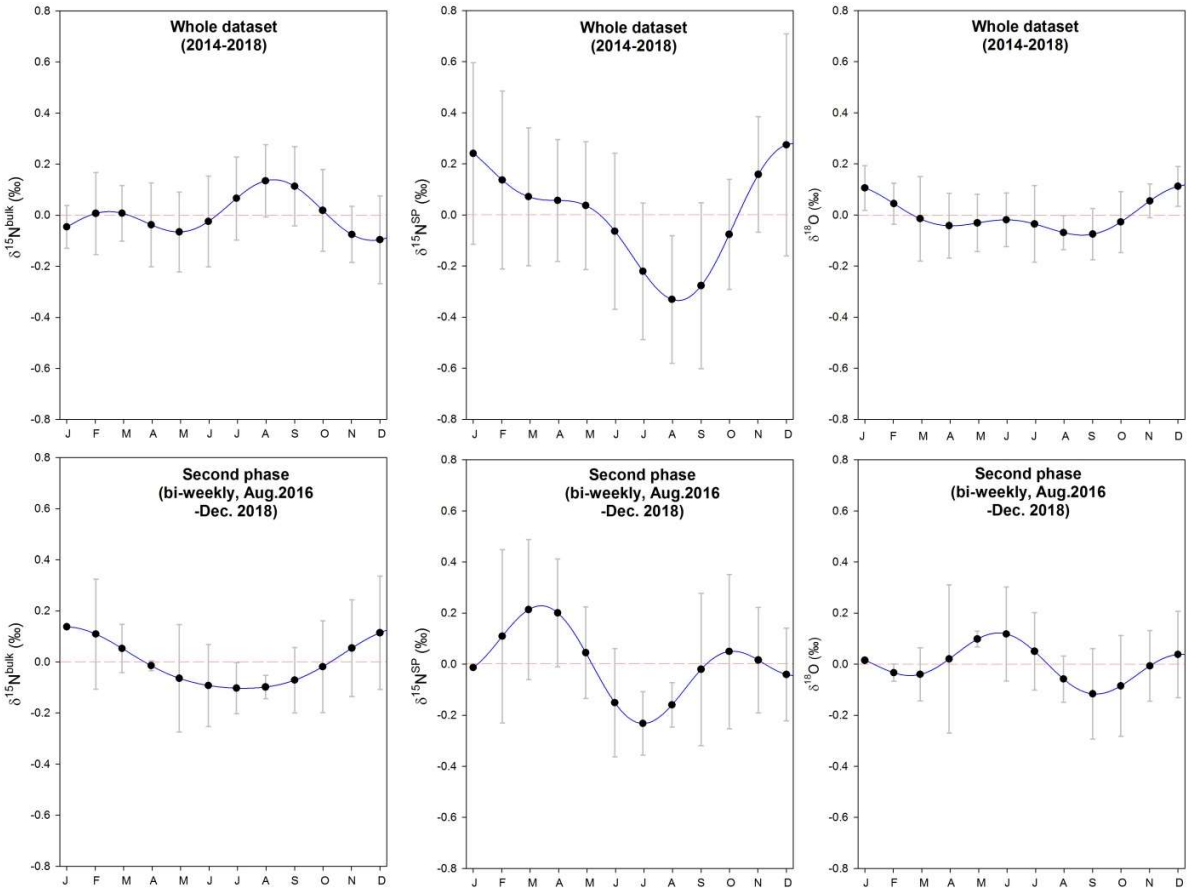

Figure 3 Seasonality of isotopic signatures of atmospheric N_2O observed at Jungfraujoch. Top panels: seasonality obtained using the whole dataset from April 2014 to December 2018; lower panels: seasonality obtained using bi-weekly data collected between August 2016 and December 2018. Red dashed lines refer to zero variability. The NLS model simulation for time-series gives the detrended seasonality, with error bars indicating one standard deviation of monthly residuals.

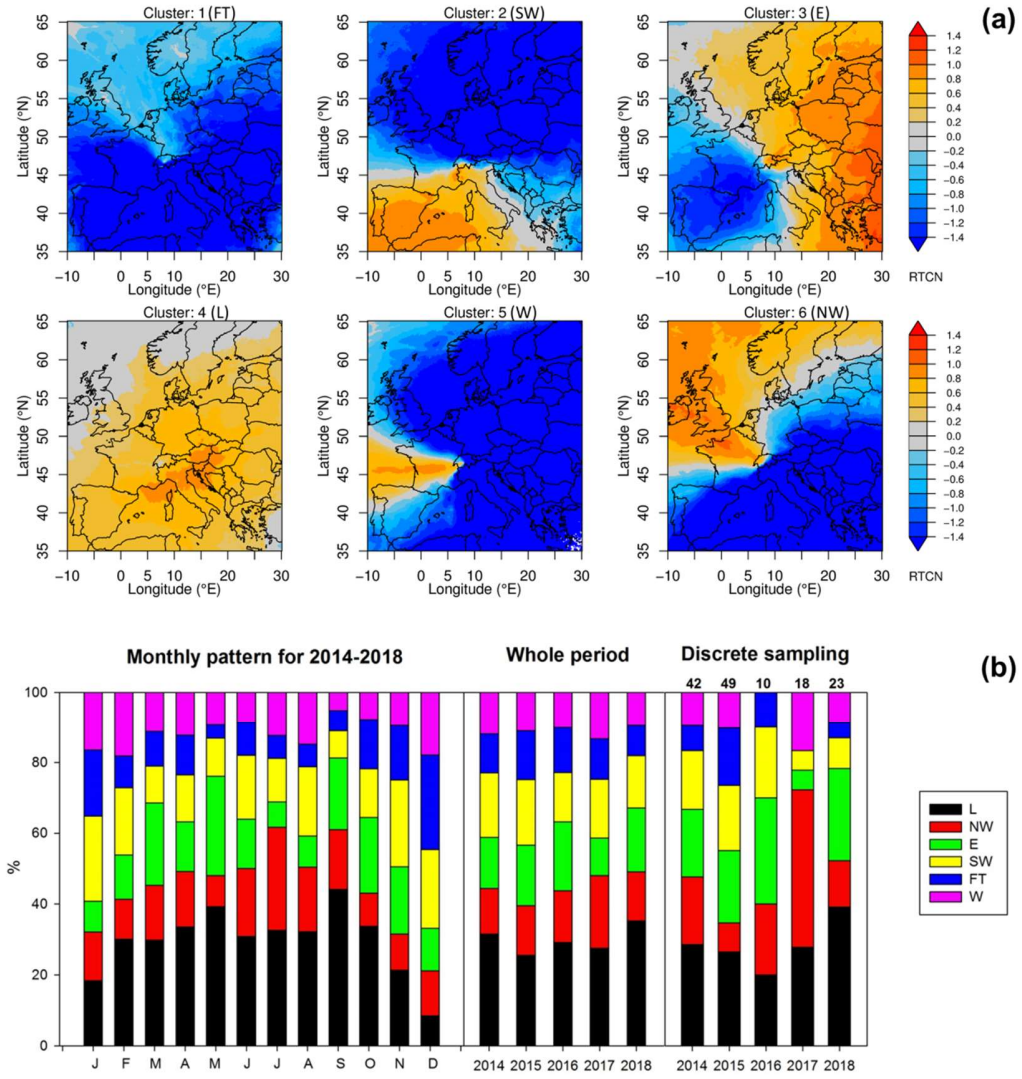

Figure 4a Clusters of air mass transport regimes for Jungfraujoch shown as normalized surface source sensitivities over our sampling period. Cluster abbreviations refer to Free Troposphere (FT), Southwest (SW), East (E), Local (L), West (W) and Northwest (NW). The normalization was done by calculating the difference between cluster average source sensitivity and whole period average source sensitivities, divided by the period average. Orange colors indicate the main source regimes in each cluster, whereas blue colors indicate little to no influence on Jungfraujoch observations. The free tropospheric cluster showed lower than average surface sensitivity everywhere.

4b Cluster frequency of air mass transport regimes (%) shown as a monthly pattern (left) and interannual patterns for the whole periods (middle) and for the periods of discrete sampling (right). Numbers above the right figure indicate the total number of discrete samples per year.

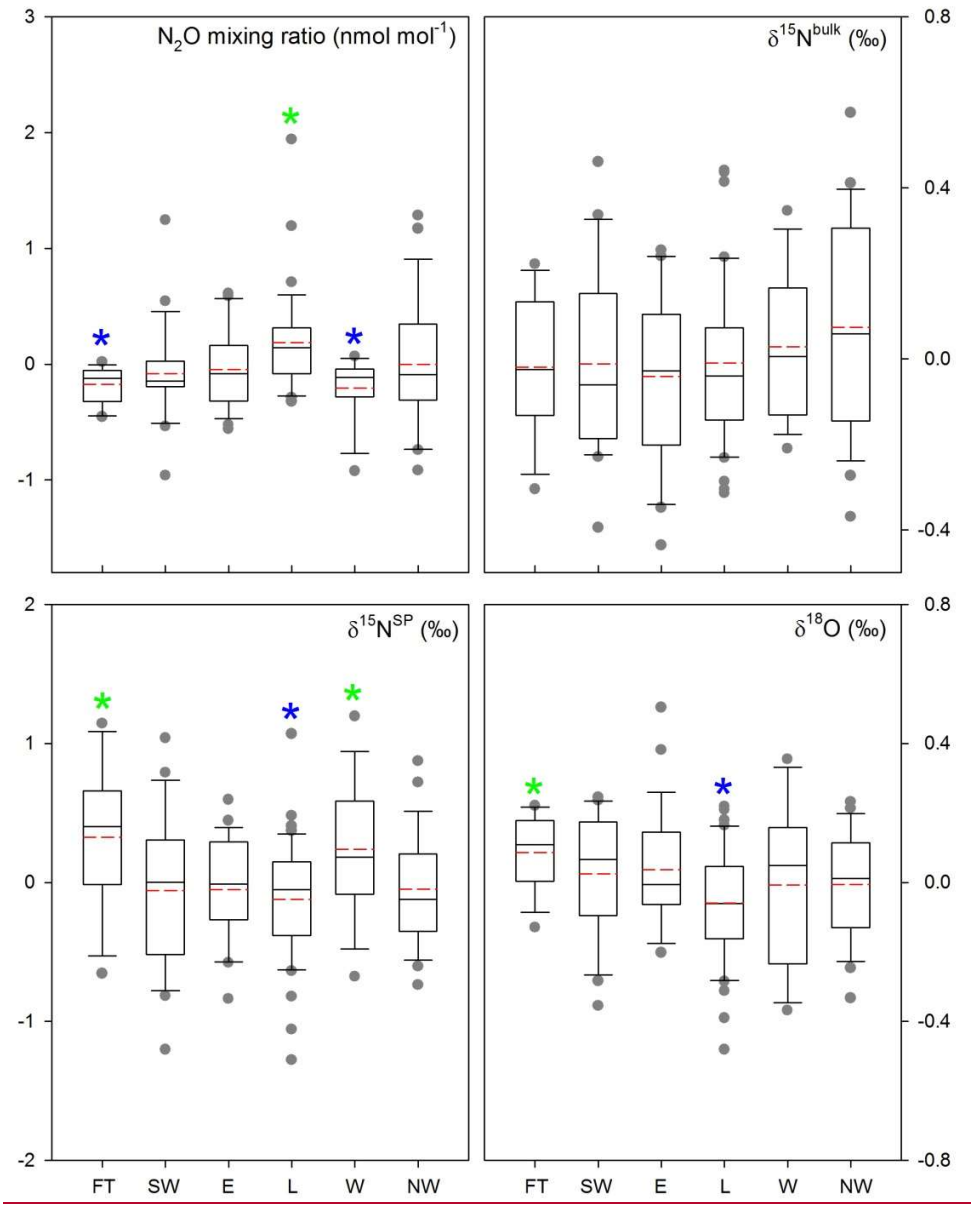

Figure 5 Comparison of N_2O mixing ratios and isotopic signatures (with linear trends removed) for the six air mass footprint clusters used in the present study. Green and blue stars indicate significantly larger and smaller values than the others, respectively; red dashed lines indicate mean levels; grey points indicate outliers.

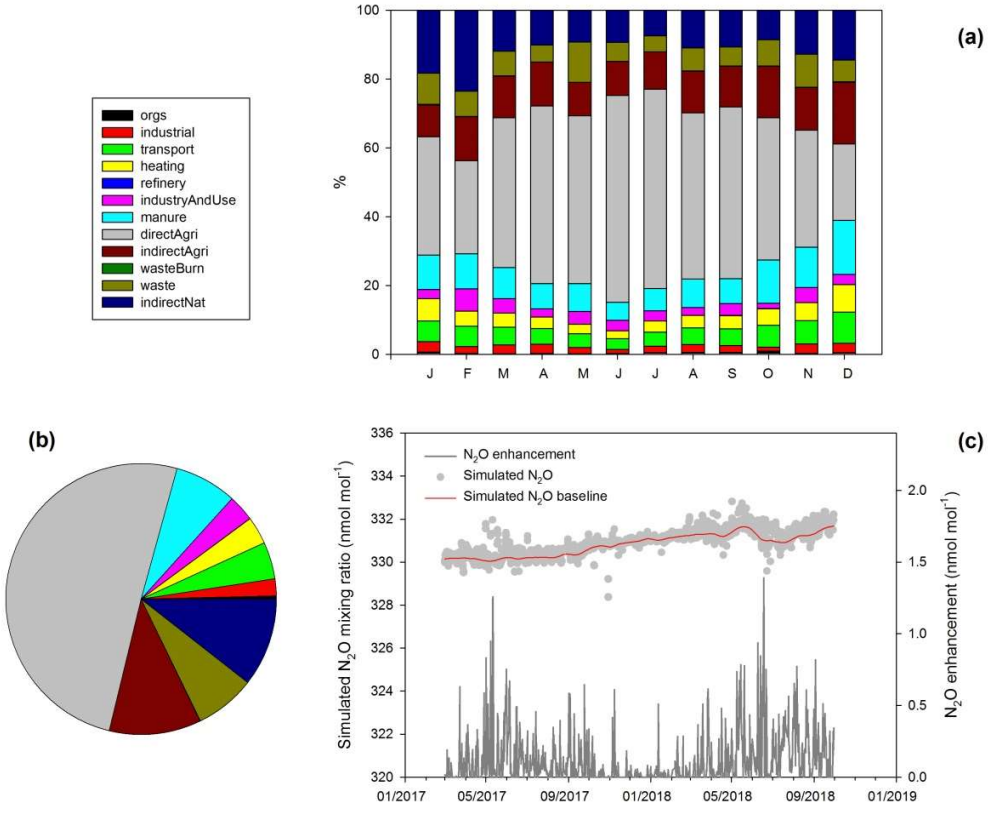

Figure ~~5a~~ 6a Mean monthly stacked-bar plots of source contributions (%) to atmospheric N_2O at Jungfraujoch derived from inversion modeling.

~~5b~~ 6b Overall contributions of N_2O sources responsible for emission to Jungfraujoch.

~~5c~~ 6c Simulated 3-hourly N_2O mixing ratios, N_2O mixing ratio baseline and N_2O enhancements in nmol mol^{-1}.

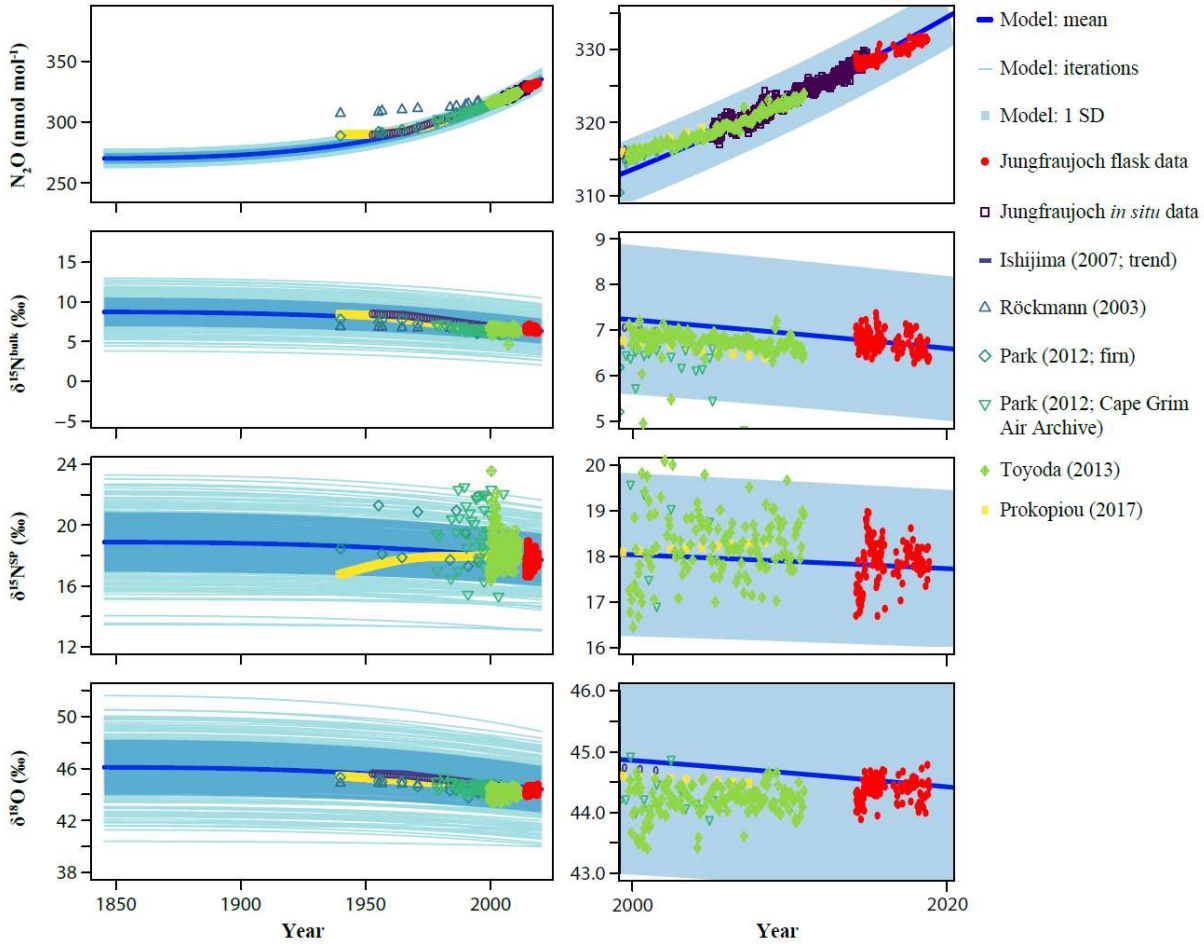

Figure ~~6~~ 7 Two-box model results showing the influence of anthropogenic emissions on N_2O mixing ratio and isotopic composition in the troposphere. Left: full time range from the start of the anthropogenic period (1845) to present day; Right: zoom to the last two decades. Isotopic measurements at Jungfraujoch were used as the only constraint of current tropospheric N_2O isotopic composition for the model. See the materials and method as well as the SI for more details and other input parameters. Atmospheric as well as firn air measurements of $\delta^{15}N^{bulk}$, $\delta^{15}N^{SP}$ and $\delta^{18}O$ from the literature are presented for comparison. Blue shaded areas indicate one standard deviation of the model iterations.